8 Hydrates in Production, Processing, and Transportation

INTRODUCTION

The objective of this chapter is provide an overview of how solid masses of hydrates (plugs) form, means of preventing and encouraging plug formation, and means of dissociating plugs once they have formed.

Unlike the other portions of the book, for example, the thermodynamic calculation methods in Chapters 4 and 5, in this chapter, conceptual pictures indicate how phenomena occur, based upon hydrate research and industrial practice. Particularly emphasized are those that have evolved during the last decade. For those who wish to do prevention calculations, several practical engineering guides are available. The engineering books by Kidnay and Parrish (2006), Carroll (2003), Makogon (1997), and Sloan (2000) prescribe hydrate calculations for the practicing engineer.

Because most of the industrial hydrate concerns have been in flow assurance, that application is emphasized. However, the concepts apply to other uses, such as gas processing and hydrated gas transport. In Section 8.1 beginning with several typical case studies of hydrate plug formation, we conclude with a conceptual overview of hydrate formation in both oil- and gas-dominated systems. Section 8.2 considers hydrate plug prevention, before considering plug remediation in Section 8.3. Then, and perhaps most important, hydrate safety is considered in Section 8.4, together with a computer program CSMPlug (on the book's CD) that provides the sole chapter exception, to enable calculations of plug remediation and safety considerations. Finally, Section 8.5 discusses concepts of gas storage and transportation.

Below are six important points to realize in this chapter:

1. Hydrate plugs and their dissociation can have major economic and safety impacts on flowline operation.
2. While the past methods of preventing hydrate plugs have been to use avoidance with thermodynamic inhibitors such as methanol or glycols, our new understanding of how plugs form, allows us to propose economic risk management (kinetics) to avoid hydrate formation. These concepts differ in type for oil-dominated and gas-dominated systems.
3. New, low dosage hydrate inhibitors (LDHIs) are being commonly used in the industry, based upon the kinetics of hydrate formation.

643

4. We can predict plug dissociation using two-sided dissociation.
5. The safety implications of plug dissociation are sometimes life-threatening, and should be an important concern.
6. It is possible to store and transport gas in hydrated form.

8.1 HOW DO HYDRATE PLUGS FORM IN INDUSTRIAL EQUIPMENT?

Considering hydrate formation and prevention, the physical conditions necessary for hydrates are

1. A hydrate guest molecule
2. Water
3. The correct conditions of temperature and pressure—usually low temperature and high pressure

Without any one of the above conditions, hydrates will not form. However, removing some of the above conditions may be impractical:

1. To remove the guest molecule (e.g., methane) may be to remove the reason for the process.
2. To use an insufficient gas pressure (typically less than 225 psia or 1.5 MPa) may decrease the energy density to a point that it is not economical.

However, it is practical to use the other thermodynamic prevention conditions:

1. Frequently the system is heated to keep it above the hydrate formation temperature at the system pressure.
2. Frequently the system has both the free water and vaporized water removed, by separation and drying the remaining gas with triethylene glycol or molecular sieves.

A second, indirect way of removing the free water is by injecting an inhibitor (typically alcohol or glycol) so that much of the free water is hydrogen bonded to the inhibitor. This reduces the water activity so that lower temperatures and higher pressures are required to form hydrates with the lower concentration of nonhydrogen bonded water, as shown in the first case study below.

In a 1999 survey of 110 energy companies, flow assurance was listed as the major technical problem in offshore development (Welling and Associates, 1999). On September 24, 2003, in a Flow Assurance Forum, Professor James Brill (2003) discussed the need for a new academic discipline called "Flow Assurance." Such a question, presented to an audience of 289 flow assurance engineers, would not have been considered in 1993, when the flow assurance community totaled a few dozen people.

Yet the statement of Professor Brill's question indicates the importance of flow assurance, particularly related to hydrates, waxes, scale, corrosion, and asphaltenes, in decreasing order of importance. In the Gulf of Mexico, for example, hydrates are considered to be the largest problem by an order of magnitude relative to the others.

Hydrate plugs do not occur in normal flowline operation due to design, but plugs are the result of three types of abnormal flowline operation:

1. When the water phase is uninhibited, as when excess water is produced, dehydrator failure, or when inhibitor injection is lost, for example, due to inhibitor umbilical failure or inhibitor pump failure.
2. Upon start-ups following emergency shut-ins, due to system component failure and recovery, such as compressor failure, without the opportunity to take inhibition steps.
3. When cooling occurs with flow across a restriction, such as in the flow of a wet gas through a choke or valve in a fuel gas line.

8.1.1 Case Study 1: Hydrate Prevention in a Deepwater Gas Pipeline

Notz (1994) noted that almost all of Texaco's efforts concerning natural gas hydrates dealt with the prevention of hydrate formation in production and transportation systems. He presented Figure 8.1 from Texaco's hydrate prevention program in a 50 mile deepwater gas pipeline, using a phase diagram similar to those discussed with Figure 4.2.

Figure 8.1 shows the pressure and temperature of fluids in a flowline at various points along the ocean floor, predicted by a multiphase flow prediction program. As a unit mass of fluid traverses the pipeline, the pressure drops normally due to friction losses associated with fluid flow. However, the temperature decrease is more interesting.

At water depths greater than 4000 ft, the ocean floor temperature is amazingly uniform at temperatures of 36–40°F. The ocean thus provides an infinite cooling medium for the warm fluids from the reservoir. In the case shown in Figure 8.1 at low pipeline distance (e.g., 7 miles) the flowing unit mass retains some residual energy (high T and high P) from the hot reservoir.

The ocean cools the fluids as they flow, including both produced water (here assumed to be salt-free) and condensed water that is always salt-free. At about 9 miles the flowing hydrocarbons and water enter the hydrate region (to the left of the line marked "hydrate formation curve"), remaining in the uninhibited hydrate envelope until mile 45. Such a distance may represent several days of residence time for the water phase (which flows slower than the hydrocarbon phases) so that hydrates would undoubtedly form, were no inhibition steps taken.

In Figure 8.1, by mile 30 the gas in the pipeline has cooled to within a few degrees of the ocean floor temperature, so that approximately 23 wt% methanol in the free water phase is required to prevent hydrate formation and subsequent
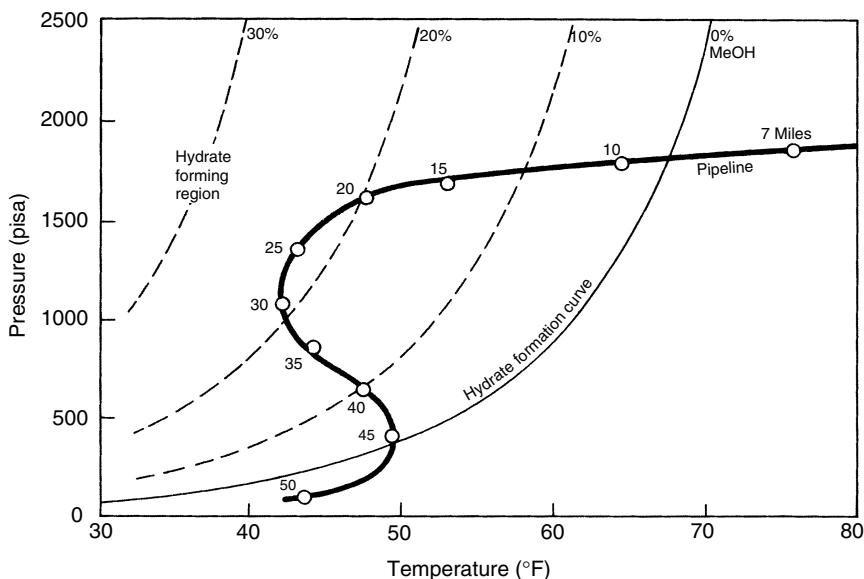
FIGURE 8.1 Typical offshore flowline system with intrusion into hydrate region. (From Notz, P.K., in *(First) International Conference on Natural Gas Hydrates*, *Ann. N.Y. Acad. Sci.*, **715**, 425, 1994. With permission.)

pipeline blockage. Methanol injection facilities are not available at the needed points (9–45 miles) along the pipeline. Instead methanol is vaporized into the pipeline at some convenient upstream point, such as a subsea well-head so that in excess of 23 wt% methanol will be present in the free water phase over the entire pipeline length.

As vaporized methanol flows along the pipeline shown in Figure 8.1, it partitions into any produced water, along with water condensed from the gas. Hydrate inhibition occurs in the free water, usually at water accumulations with some change in geometry (e.g., a riser, bend, or pipeline dip along an ocean floor depression) or some nucleation site (e.g., sand, weld slag, etc.).

Hydrate inhibition occurs in the aqueous liquid, rather than in the vapor or hydrocarbon liquid phases. While a significant portion of the methanol partitions into the water phase, a significant amount of methanol either remains with the vapor or partitions into any liquid hydrocarbon phase. Although the methanol mole fraction in the vapor or liquid hydrocarbon may be low relative to the water phase, the large amounts (phase fractions) of vapor and liquid phases will cause a substantial amount of inhibitor loss.

In Figure 8.1 Notz notes that the gas begins to warm (from mile 30 to mile 45) with shallower, warmer water conditions. From mile 45 to mile 50, however, a second cooling trend is observed due to Joule–Thomson expansion. The methanol exiting the pipeline in the vapor, aqueous, and condensate phases is usually not recovered, due to the expense of separation.

Note that regular methanol (or monoethylene glycol) injection is used only with gas-dominated systems. In oil-dominated systems the higher liquid heat capacity allows the system to retain reservoir heat, so that insulation maintains sufficient temperatures to prevent hydrate formation. Thermodynamic inhibitor is normally only injected for planned shutdowns in oil-dominated systems.

8.1.2 Case Study 2: Hydrates Prevention via Combination of Methods

As a summary of the thermodynamic hydrate prevention methods, consider the steps taken to prohibit hydrates in the Dog Lake Field export pipeline in Louisiana, by Todd et al. (1996) of Texaco. During the winter months hydrates formed in the line, which traverses land and shallow water (a marsh).

Hydrate formation conditions, shown in Figure 8.2 are calculated via the methods of Chapters 4 and 5 with 0, 10 and 20 wt% methanol in the water phase. The Dog Lake gas composition is: 92.1 mol% methane, 3.68% ethane, 1.732% propane, 0.452% i-butane, 0.452% n-butane, 0.177% i-pentane, 0.114% n-pentane, 0.112% hexane, 0.051% heptane, 0.029% octane, 0.517% nitrogen, 0.574% carbon dioxide.

The pipeline pressure and temperature, calculated using PIPEPHASE®, were superimposed on the hydrate formation curve shown in Figure 8.3. Gas leaves
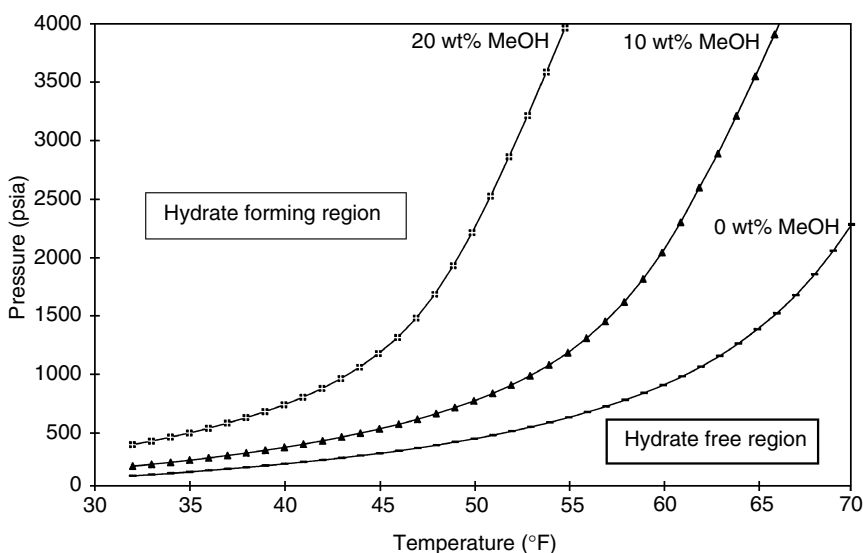

FIGURE 8.2 Dog Lake gas hydrate formation curves with methanol in free water phase. (From Todd, J.L., et al., *Reliabilty Engineering—Gas Freezing and Hydrates*, Texaco Company Hydrate Handbook (1996). With permission.)
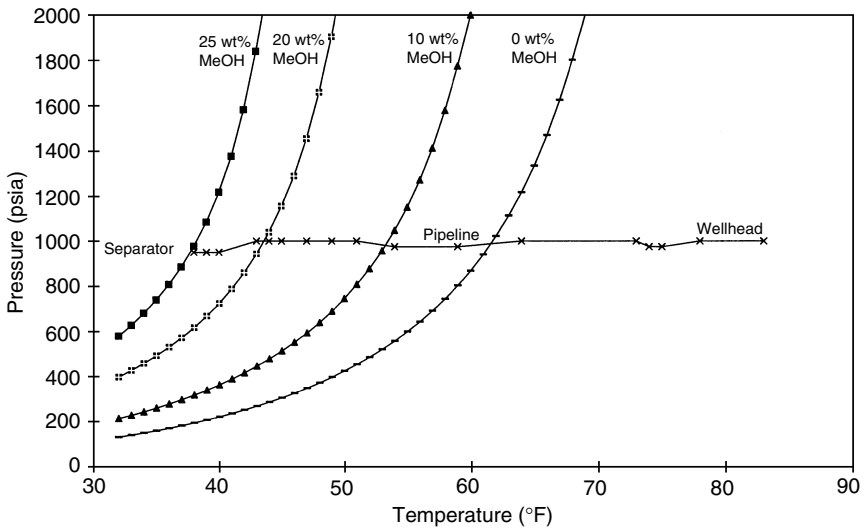
FIGURE 8.3 Normal Dog Lake flowline conditions indicating the need for methanol. (From Todd, J.L., et al., *Reliabilty Engineering—Gas Freezing and Hydrates*, Texaco Company Hydrate Handbook (1996). With permission.)

the wellhead at 1000 psia and 85°F, far from hydrate forming conditions. As the gas moves down the pipeline, it is cooled toward ambient temperatures. Once the temperature reaches approximately 62°F, hydrates will form, so methanol must be added to avoid blockage. The figure shows pipeline conditions and the hydrate formation curves for various concentrations of methanol, indicating that 25 wt% methanol in the free water phase is needed to inhibit hydrates.

Despite large quantities of methanol injection for hydrate prevention, 110 hydrate incidents occurred in the Dog Lake line during the winter of 1995–1996 at a remediation cost of $323,732, not counting lost production. Combinations of four alternative hydrate prevention methods were considered: (1) burying the pipeline, (2) heating the gas at the wellhead, (3) insulating the pipeline, and (4) methanol addition. The first three methods were intended to maintain sufficiently high temperatures to prevent hydrate formation, while the last method effectively inhibited free water, via hydrogen bonding with methanol. The details of each prevention measure are considered below.

8.1.2.1 Burying the pipeline

Portions of the Dog Lake pipeline were built over a stretch of marsh. The exposure to winter ambient temperatures caused rapid reductions in the gas temperature. Burying the pipeline would protect it from low environmental temperatures due to the higher earth temperatures. Figure 8.4 shows the increase in the pipeline
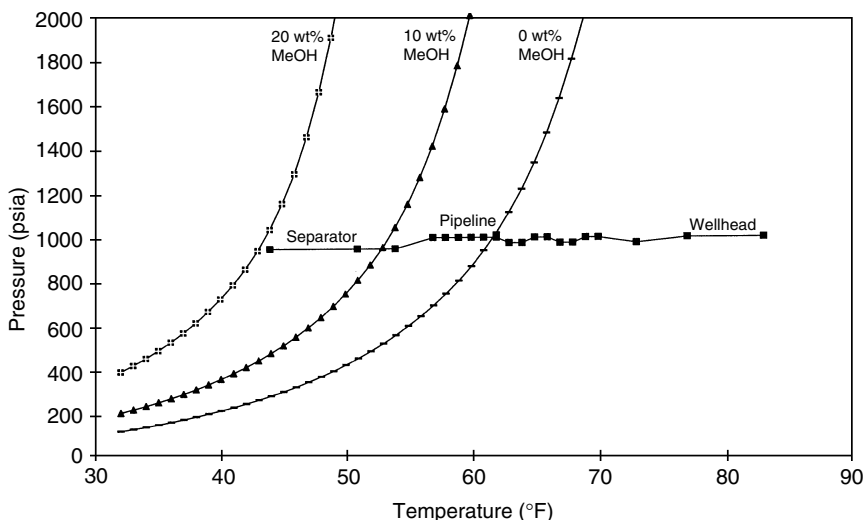
FIGURE 8.4 Dog Lake line burial increased the discharge temperature and reduced the amount of methanol. (From Todd, J.L., et al., *Reliabilty Engineering—Gas Freezing and Hydrates*, Texaco Company Hydrate Handbook (1996). With permission.)

discharge temperature after the exposed areas were buried, relative to the exposed line in Figure 8.3. With pipeline burial, the need for methanol in the water phase was reduced from 25 wt% (Figure 8.3) to less than 20 wt% (Figure 8.4).

8.1.2.2 Line burial with wellhead heat addition

Line heaters could be installed at the wellhead to increase the inlet gas temperature from 85°F to 125°F. Figure 8.5 shows the pipeline temperature increase caused by the combined prevention methods of burial and wellhead heating. Use of these two methods permitted the methanol concentration in the free water phase to be reduced to approximately 14 wt% to prevent hydrate formation in the line. It should, however, be noted that heating may increase the amount of corrosion in the line.

8.1.2.3 Burial, heat addition, and insulation

In addition to line burial and the addition of heat at the wellhead, insulation of exposed areas near the wellhead maintained higher pipeline temperatures, thereby reducing the amount of methanol needed for hydrate inhibition. Figure 8.6 displays the temperature increase in the buried and heated pipeline when exposed pipes were insulated. A combination of the methods causes the pipeline fluid to be outside the hydrate formation region (to the right of the curve marked 0 wt% MeOH), and methanol addition is no longer needed.
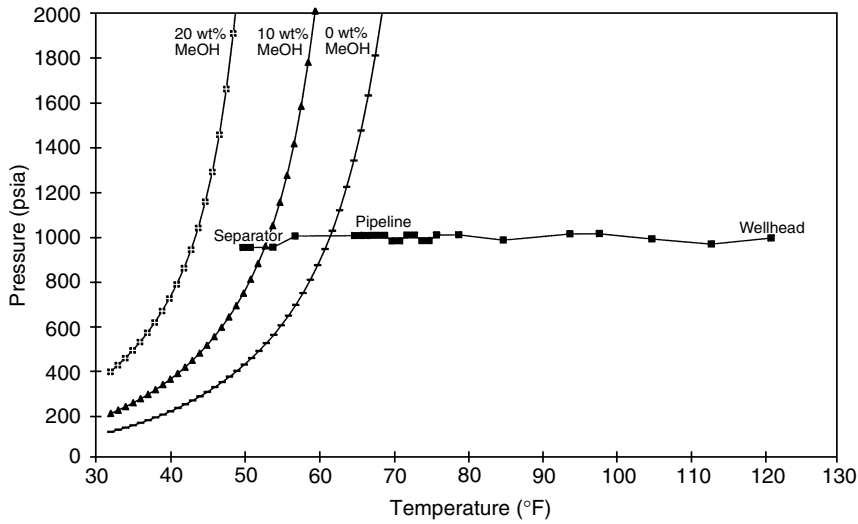
FIGURE 8.5 Dog Lake line burial and inlet heating reduces the need for methanol. (From Todd, J.L., et al., *Reliabilty Engineering—Gas Freezing and Hydrates*, Texaco Company Hydrate Handbook (1996). With permission.)

FIGURE 8.6 Dog Lake line burial, inlet heating, and insulation removes system from hydrate region. (From Todd, J.L., et al., *Reliabilty Engineering—Gas Freezing and Hydrates*, Texaco Company Hydrate Handbook (1996). With permission.)
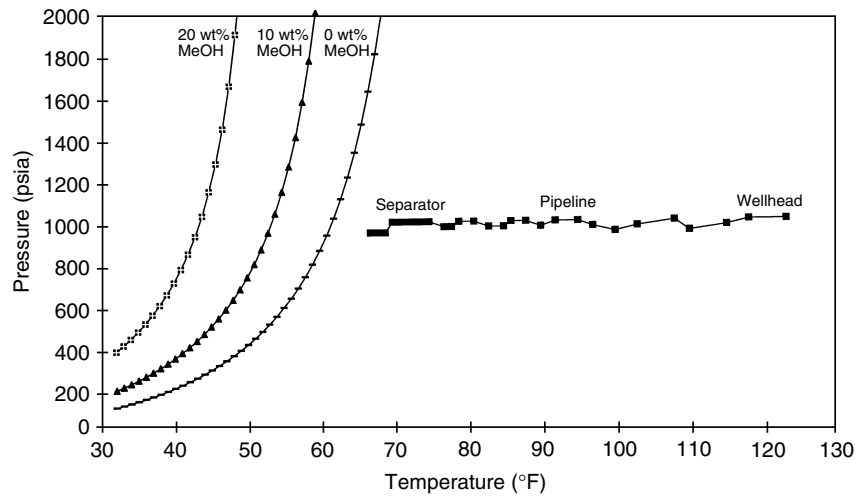
8.1.2.4 Methanol addition alternative

Continued methanol injection could be done at a cost of approximately $1.50–2.00 per gallon during the 1996–1997 winter. Since methanol recovery is problematic,

methanol is normally considered an operating cost. In addition, refineries have put restrictions on methanol concentrations in condensate and this further decreases the economics of methanol injection.

This case study illustrates how combinations of pipeline burial, insulation, heating, and methanol injection can be used to prevent hydrates. The selection of the hydrate prevention scheme(s) is then a matter of balancing capital against operating costs.

8.1.3 Case Study 3: Hydrate Formation via Expansion through Valves or Restrictions

When water-wet gas expands rapidly through a valve, orifice or other restriction, hydrates form due to rapid gas cooling caused by adiabatic (Joule–Thomson) expansion. Hydrate formation with rapid expansion from a wet line commonly occurs in fuel gas or instrument gas lines. Hydrate formation with high pressure drops can occur in well testing, start-up, and gas lift operations, even when the initial temperature is high, if the pressure drop is very large.

Figure 8.1 shows the pressure and temperature of a pipeline production stream during normal flow with entry into the hydrate formation region. If the gas expands more rapidly, the normal pipeline cooling curve of Figure 8.1 will take on a much steeper slope, but the hydrate formation line remains the same. Two rapid Joule–Thomson expansion curves for a 0.6 gravity gas are shown in Figure 8.7. Intersections of the gas expansion curves with the hydrate formation line (bounding the shaded area) limits the expansion discharge pressures from two different high initial pressure/temperature conditions.

In Figure 8.7, the curves determine the restriction downstream pressure at which hydrate blockages will form for a given upstream pressure and temperature. Gas A expands from 2000 psia and 110°F until it strikes the hydrate formation curve at 700 psia (and 54°F), so 700 psia represents the limit to hydrate-free expansion. Gas B expands from 1800 psia (120°F) to intersect the hydrate formation curve at a limiting pressure of 270 psia (39°F). In expansion processes while the upstream temperature and pressure are known, the discharge temperature is almost never known, but the discharge pressure is normally set by a downstream vessel or pressure drop.

Cooling curves such as the two in Figure 8.7 were determined for constant enthalpy (or Joule–Thomson) expansions, obtained from the First Law of Thermodynamics for a system flowing at steady-state, neglecting kinetic and potential energy changes:

$$\Delta H = Q + W_s \tag{8.1}$$

where ΔH is the enthalpy difference across the restriction (downstream–upstream), while Q represents the heat added, and W_s is shaft work done at the restriction. Restrictions (e.g., valves or orifices) have no shaft work, and because rapid flow
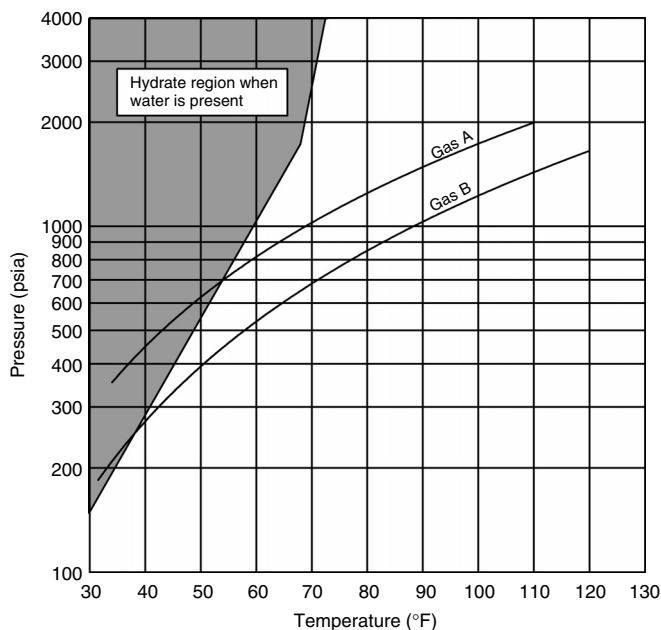
FIGURE 8.7 Expansion of two gases into the hydrate formation region. (From Katz, D.L., *Trans AIME*, **160**, 140 (1945). With permission.)

approximates adiabatic operation (limited heat transfer); both W_s and Q are zero, resulting in constant enthalpy ($\Delta H = 0$) operation on expansion.

Due to the constant enthalpy requirement, rapid gas expansion with pressure lowering normally results in cooling. Because of the constraint that the enthalpy (roughly a flow-corrected energy) must be equal on both sides of the valve, a lower pressure gas (higher enthalpy) downstream of the valve, must be compensated by a lower temperature (lower enthalpy). So Figure 8.7 for fluid expansion through a valve has a steeper slope than normal flow along a pipeline (Figure 8.1) that has heat transfer (Q) with the surroundings, which are typically around 40°F.

To prevent hydrate formation in expansion on the downstream side of a valve, the most common method is to inject methanol or glycol before the value, removing the hydrate formation (shaded) region to the left of Figure 8.7 from the expansion conditions. Alternatives include heating the inlet gas or limiting the downstream pressure.

In concluding this case study, it should be recalled that Section 4.2.1.1 provides the hand calculation limits to Joule–Thomson expansion, through Figures 4.7 through 4.9. The computer program CSMGem on the CD supplied with this book also provides a method for calculation of expansion limits, as shown in the User's Examples in Appendix A, and in the User's Guide found on the CD accompanying this volume.
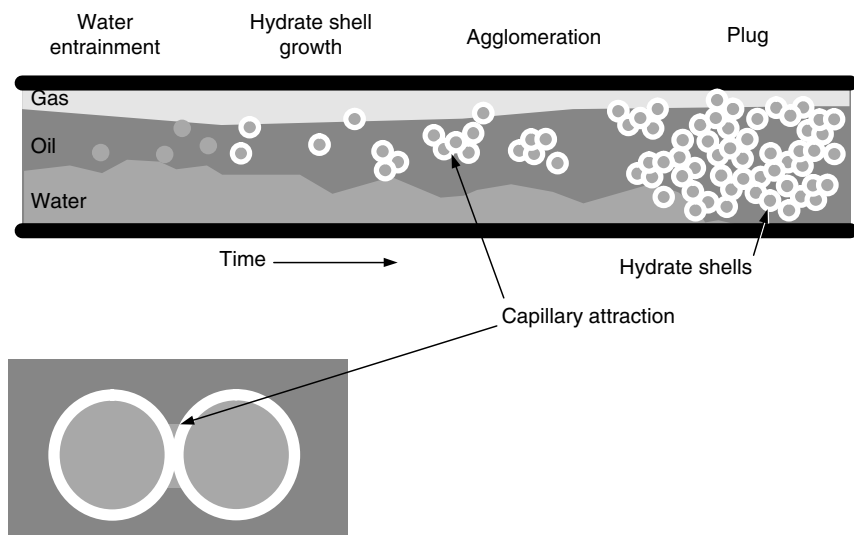
FIGURE 8.8 **(See color insert following page 390.)** Plug formation via aggregation in an oil-dominated system. (From Turner, D.J., *Clathrate Hydrate Formation in Water-in-Oil Dispersions*, Ph.D. Thesis, Colorado School of Mines, Golden, CO (2004). With permission.)

8.1.4 Conceptual Overview: Hydrate Plug Formation in Oil-Dominated Systems

Figure 8.8 gives a conceptual figure of hydrate formation in an oil-dominated pipeline. This figure is an extension of the hypothesis originally proposed by Norsk Hydro (Lingelem et al., 1994) and has gained some acceptance in the industry.

In Figure 8.8 six steps are involved in hydrate plug formation:

1. The water phase is emulsified within the oil phase. Usually the oil phase fraction is much greater than the water phase fraction, so the large majority of oil production involves a water within oil (W/O) emulsion. The water droplet size is typically tens of microns (μm).
2. A thin (perhaps smaller than 6 μm thick) hydrate shell grows around the water droplets, from small gas molecules dissolved in the oil phase. Initially this hydrate shell is extremely malleable, so much so the hydrate-encrusted droplet will extrude through screens, for example.
3. While they are malleable, these hydrate shells form a diffusional barrier between the hydrocarbon and water phases. The shells do not usually become very thick, except at long times—periods of days.
4. Capillary forces of attraction cause the hydrate-encrusted droplets to agglomerate. These capillary forces are a strong function of temperature; at low temperatures the forces decrease between the particles, as measured by Taylor (2006).

5. As the hydrated particles agglomerate, the effective viscosity increases dramatically, and spikes in the flowline pressure drop occur with time, indicating agglomeration and breakage of hydrate masses. Finally the agglomerate becomes sufficiently large to increase the pressure drop so that flow is stopped. This point is normally taken as a hydrate plug, causing flow to be shut in.

6. As the plug sits for a longer period of time, the masses anneal and the plug becomes more solid-like, with less flexibility. That is, both intra- and interparticle growth occurs. This annealing process is not shown in Figure 8.8.

The simplified conceptual picture in Figure 8.8 has important implications for flow assurance. For example, the model's implication is that hydrate agglomeration (not the kinetics of shell growth) is the limiting factor in plug formation. If one could determine a means of preventing agglomeration, such as antiagglomerants (AAs) (Mehta, et al., 2003) or cold flow (Wolden, et al., 2005), one could allow the hydrates to form and flow without obstructing the pipeline. There is significant evidence that such situations normally occur in flowlines in Brazil (Palermo et al., 2004), where natural AAs exist in oils.

8.1.5 Conceptual Overview: Hydrate Formation in Gas-Dominated Systems

Hydrate formation in a gas-dominated system is thought to differ significantly from formation in oil-dominated systems. In gas systems, there is much less liquid (both hydrocarbon and water), so that the W/O emulsion concept may not apply. Instead a concept may apply as shown in Figure 8.9.

The bottom portion of Figure 8.9 gives the concept of hydrate formation in a gas-dominated system, while the top portion shows the line pressure (note the semi-logarithmic scale) before a hydrate plug point as a function of time in the pipeline, upstream of a water/hydrate accumulation, corresponding to the lower conceptual portions of the figure. The bottom conceptual picture is a second extension of a picture originally proposed by Lingelem et al. (1994). The pressure data shown were obtained just before the location of hydrate formation at the Werner–Bolley gas line in Wyoming by Hatton and Kruka (2002).

Figure 8.9 suggests five steps for hydrate formation in a gas-dominated line:

1. Water in the pipeline (at Point A) is due to both produced water, and condensed water from the gas.

2. Hydrates originally form at the walls of the pipe (Point B) via vapor deposition and/or splashing of water with subsequent conversions. The wall is the radial point of lowest temperature, and consequently the point of hydrate deposition due to heat transfer with the outside environment, which is at a lower temperature than the gas.

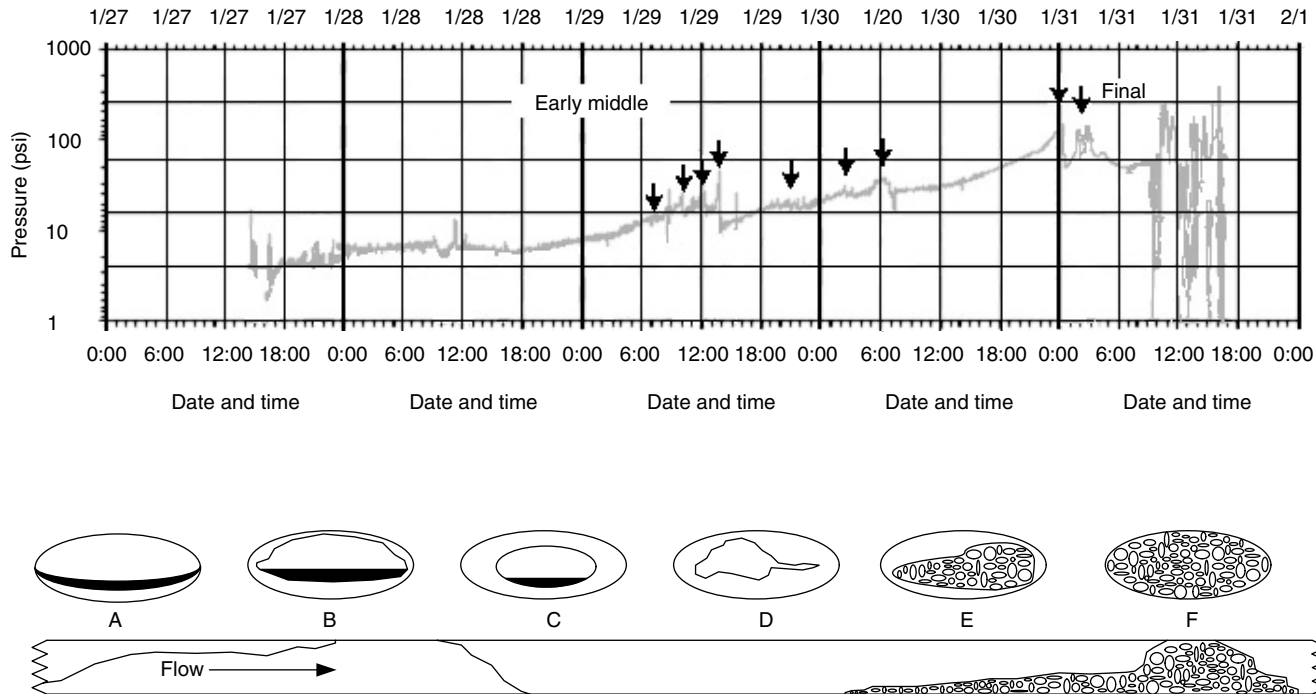**FIGURE 8.9** Hydrate blockage formation (bottom) and corresponding pressure buildup (top) in a gas-dominated pipeline (upper figure From Hatton, G.J., Kruka, V.R., *Hydrate Blockage Formation—Analysis of Werner Bolley Field Test Data*, DeepStar CTR 5209-1, 2002; lower figure modified from Lingelem, M.N., et al., in *(First) International Conference on Natural Gas Hydrates*, *Ann. N.Y. Acad. Sci.*, **715**, 75 (1994). With permission.)

3. As the hydrate deposition on the wall becomes thicker (Point C), narrowing of the flow channel occurs. The deposition forms irregularly (Point D) so that a nonconcentric annulus increases the pipeline pressure drop. Steps 1–3 are in the stages of hydrate plug formation marked "early" in the top of Figure 8.9, with a gradual upstream pressure increase.

4. At Point E in the bottom of Figure 8.9, the hydrate wall deposit can no longer bear the stress imposed by a combination of the fluid passing by together with the hydrate deposit weight, and hydrate sloughs from the wall. These sloughs are marked by a decrease in the upstream pressure, at each of the arrows in the top of Figure 8.9 in the portion marked "middle."

5. As the sloughed particles travel downstream, they bridge across the flow channel (Point F) to form a plug, with the corresponding upstream pressure spikes as shown in the "final" period of the top of Figure 8.9.

The above simplified picture has important implications for flow assurance in gas lines, as shown by the gas line operation in the case studies of Section 8.2.

8.2 How are Hydrate Plug Formations Prevented?

The five studies of hydrate formation given in Section 8.1 are of two types. The first three case studies show thermodynamic (time-independent) methods to prevent plug formation. However, the second type provides a closer, mechanistic look at the physical kinetics (time-dependent) hydrate formation and agglomeration. A goal of this section is to show how these two methods provide two different methods of plug prevention.

Avoidance of the hydrate formation thermodynamic conditions of temperature, pressure, or inhibitor concentration, makes it impossible for plugs to form. The calculations of thermodynamic conditions can be made with acceptable accuracy. Using the methods presented in Chapters 4 and 5 along with the CD program CSMGem provided with this book, the temperature, pressure, and inhibitor concentrations can be calculated respectively, to within 2°F, 10% in pressure and 3% of inhibitor concentration. Since the discovery of hydrate flowline plugs in 1934, such thermodynamic methods have served to provide the major method of flow assurance.

However, as mankind has exhausted the most accessible hydrocarbon supplies, more severe conditions (e.g., higher pressures, lower temperatures, and higher acid gas contents) caused thermodynamic prevention means to be less acceptable economically. The following two case studies illustrate the fact that thermodynamic inhibition is becoming very expensive.

8.2.1 Case Study 4: Thermodynamic Inhibition Canyon Express and Ormen Lange Flowlines

1. At start-up in September 2002, the Canyon Express development in the Gulf of Mexico was the world's deepest, with the three field locations in

6500–7200 ft of sea water (Hare and Case, 2003). Due to the extreme depth, large amounts of methanol injection necessitated an unusual distillation methanol recovery. Without methanol recovery, the Canyon Express maximum design of 1000 BPD of water production requires 1 million dollars of methanol injection (at U.S.$1/gal methanol) every 16 days.

2. The Ormen Lange gas field (Wilson et al., 2004), offshore of northern-Norway, when it commences production in 2016, will have two unusual features: (1) flow of fluids uphill against a seabed gradient of 26% and (2) an unusual ocean bottom temperature of 30°F due to subsea currents. Typical deepwater temperatures are around 40°F (well above 32°F, the freezing point of water), and such a low temperature at Ormen Lange means that any water produced could form ice, as well as hydrates. Extra precautions, must be taken because an ice plug is much more problematic to remove than a hydrate plug (which can be removed by depressurization). The estimated maximum monoethylene glycol injection needed is 26,500 ft^3/d, with a capacity of 53,000 ft^3/d. As a result, when the Ormen Lange inhibition system is first charged, the amount of monoethylene glycol will require 67% of the world's annual production capacity (Wilson, Personal Communication, March 15, 2004).

The above two examples serve to illustrate that more severe conditions of gas recovery require large expense in thermodynamic inhibitors. The high pressure and high water production at Canyon Express and the steeply upward sloping lines and subfreezing temperatures of Ormen Lange are harbingers of more severe conditions in the future. There are some cases in which the cost of hydrate inhibitors determine the project viability.

A fair question is, "If industry always recovers from infrequent blockages, what is the economic incentive to justify the risk of very infrequent blockages?" The answer is complex, including technical disciplines, statistics, economics, and risk management.

Forty-six case studies of hydrate plug formation and remediation are recorded in *Hydrate Engineering* (Sloan, 2000). In every case, hydrate plugs were remediated. In addition, a rule of thumb is that most of the offshore flowline shut-ins are less than the 10 h "no touch" time, which requires no antihydrate operation before restart (J.E. Chitwood, Personal Communication, August 1, 2003). However, hydrate prevention methods are very expensive, as shown in the above Canyon Express and Ormen Lange examples, or in the fact that deepwater insulation costs are typically U.S.$1 million per kilometer of flowline.

In the future, economic risk evaluation will guide the hydrate-plugging prevention philosophy. It is important to note that phase equilibria thermodynamics provide the current paradigm of hydrate avoidance, but risk management is in the domain of time-dependent phenomena or physical hydrate kinetics. The experience base with hydrate plugs and their remediation impacts the economic need for large amounts of insulation and/or thermodynamic inhibitors.

While accurate thermodynamic predictions (as in Chapters 4 and 5) enable avoidance via use of inhibitors such as methanol, risk management is enabled by operating experience and by kinetic predictions. Hydrate thermodynamic predictions can provide avoidance techniques, but kinetic predictions are required to provide techniques of risk management.

Lacking an acceptable hydrate kinetics model, however, the leaders in deepwater multiphase flow operations have moved to risk evaluation technology, again using the engineering method of using the best technology, past operating experiences, and taking small risks in new designs. There are several examples to illustrate risk evaluation or kinetics in flowline design: (1) hydrate kinetic inhibitors, (2) antiagglomerants, and (3) hydrate plug dissociation. The use of each of the three methods is affected by the time-wise kinetics of hydrate formation and dissociation. Each is discussed in examples that follow.

An operating example of time-dependence is presented as an industrial finding, pointing out the need for hydrate kinetics.

8.2.2 Case Study 5: Under-Inhibition by Methanol in a Gas Line

Flow assurance engineers for a major energy company (Mehta et al., 2003) indicate that for a two year periods, one of their offshore gas flowlines operated well inside the hydrate formation region. The problem arose from increased water production (to > 1000 BPD) over the field life, with limited methanol delivery. Their approach was to inject as much methanol as possible, in the knowledge that they were under-inhibiting the system. Due to under-inhibition, there was a gradual increase in the pressure drop (ΔP) in the line over a period of about 2 weeks, indicating a hydrate build-up on the walls.

Upon increase of ΔP over two weeks, gas production was gradually reduced, while continuing to inject methanol at the same (maximum) rate as before. By reducing gas (and thus the water) production, the methanol concentration increased. A higher methanol concentration melted hydrate that had formed in the line. After allowing the high concentration methanol to sweep the hydrates for some time, the pressure drop returned to normal and production was gradually ramped to its original gas rate. The 2 week cycle then was repeated.

This strategy was successful in extending the field life by almost 2 years. This is one key example of the risk management philosophy, enabled by operating experience on the platform. The hydrate plug prevention technique in this case study is time-dependent and should be contrasted with thermodynamic (time-independent) inhibition methods in Case Study 4 of Canyon Express and Ormen Lange.

While accurate thermodynamic predictions enable avoidance via use of thermodynamic inhibitors such as methanol or glycol, hydrates risk management is enabled by experience in the form of experiments, both in the field and in the laboratory. This is because, as indicated in Chapter 3, there is no comprehensive, predictive hydrate kinetic theory that can be accurately invoked at high hydrate

concentrations. The very best work in hydrate kinetics comes from the laboratory of Bishnoi over the last three decades. However, that work was confined to low hydrate concentrations, due to the need to eliminate confounding heat and mass transfer phenomena. In pipelines and other processes, heat and mass transport phenomena can commonly limit hydrate formation more than kinetics.

The following sections present three examples of kinetic phenomena: (1) kinetic inhibitors, (2) antiagglomerants (AAs), and (3) hydrate plug remediation. These kinetic phenomena were determined by field and laboratory observations. They also point to the need for a comprehensive kinetics theory, from which hydrate nucleation and growth can be predicted for industrial utility.

As shown in Chapter 3 and in Figure 8.8, the three steps to hydrate plug formation are (1) nucleation of hydrate films, (2) growth of hydrate films around water droplets or along the wall, and (3) agglomeration of hydrated particles to form plugs. Kinetic hydrate inhibitors (KHIs, also known as KIs) and AAs, both falling under the general nomenclature of low dosage hydrate inhibitors (LDHIs), which are typically lower in concentration than 1 wt%, provide chemical approaches to all three of the plug formation mechanisms. While kinetic inhibitors focus on the first two means of prevention, AAs deal with the third means. It should be noted that in addition to the chemical means of hydrate plug prevention, there are flow means of doing so, but this evolving technology is not discussed here.

A major thrust of the research on LDHIs is driven by concern for the environment—for chemicals with high biodegradability. The Norwegian Pollution Authority requires that all new chemicals used offshore must have a biodegradability of higher than 60%, while British environmental authorities require a biodegradability of greater than 20% for new offshore chemicals. For example, although kinetic inhibitors such as those based on PVCap (see description below) and water-soluble polymers have low toxicity, neither kinetic inhibitors nor AAs can be used in the Norwegian sector of the North Sea, while normal PVCap has a biodegradability below the British requirements. Grafted polymers have been developed to help increase the biodegradability of the kinetic inhibitor polymer (Maximilian et al., 2005). In other places in the world where restrictions are not so stringent, kinetic inhibitors and AAs have wider use.

8.2.3 Kinetic Hydrate Inhibition

Kinetic inhibitors are low molecular weight polymers dissolved in a carrier solvent and injected into the water phase in pipelines. These inhibitors bond to the hydrate surface and prevent plug formation for a period longer than the free water residence time in a pipeline. Liquid hydrocarbons may or may not be present for this prevention method to be effective. Water and small hydrate crystals are removed at a platform or onshore. Kinetic inhibitors are limited at long times, low temperatures, and high pressures because with sufficient time, the crystal growth is significant enough to cause line plugs.

However, there is a limit to the effectiveness of the inhibitors, commonly taken to be a subcooling (ΔT = temperature below the equilibrium temperature)
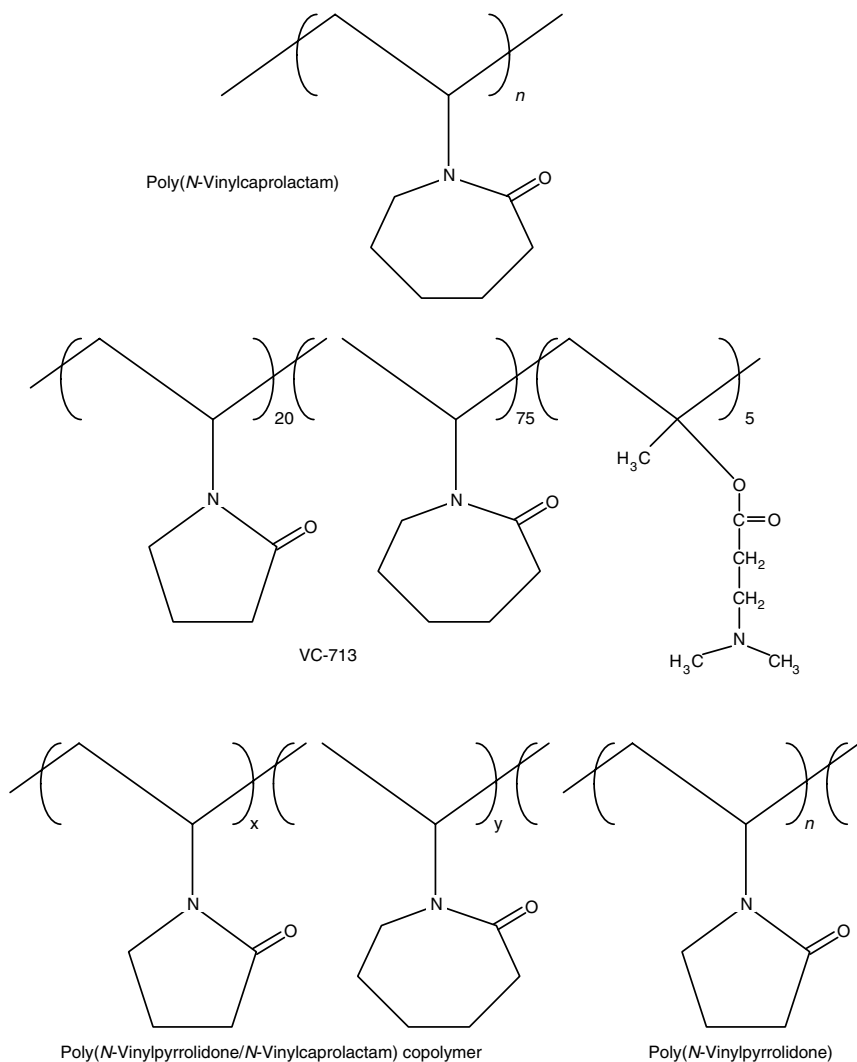
FIGURE 8.10   Hydrate kinetic inhibitors. Unless indicated, every angle is the location of a carbon atom and the appropriate number of hydrogens.

of 20°F. These kinetic inhibitors have been shown to be active at significantly lower concentrations than thermodynamic inhibitors, that is, about 0.5–2.0 wt% versus 40–60 wt%.

    Examples of kinetic inhibitor chemicals are shown in Figure 8.10. In the figure, each inhibitor is shown with a polyethylene backbone, from which a pendant group (typically a ring compound with an amide [—N—C═O] linkage) is suspended. There are several types of kinetic inhibitors, and due to proprietary

$$\Delta T < \frac{4\sigma}{C \cdot L}$$

FIGURE 8.11   One mechanism for kinetic inhibition $\Delta T \leq 4\sigma/C{\cdot}L$.

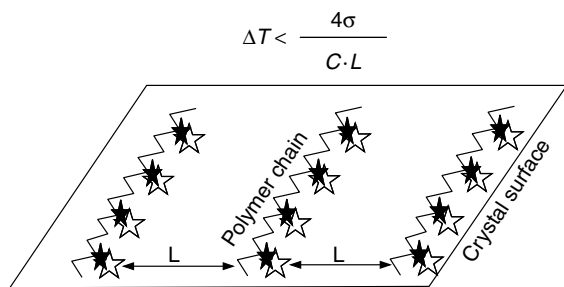concerns, only a few in the literature are discussed to show the principles involved. The reader is referred to the review by Kelland (2006) for a more detailed overview.

The definitive hydrate kinetic inhibition mechanism is not yet available. Some work suggests that the mechanism is to prevent hydrate nucleation (Kelland, 2006). However, a significant amount of evidence suggests that hydrate kinetic inhibitors inhibit the growth (Larsen et al., 1996). However, this apparent conflict is due to the definition of the size at which crystal nucleation stops and growth begins. To resolve this confusion, one may consider growth to occur after the critical nucleus size is achieved.

As indicated in Figure 8.11, the subcooling ΔT is directly proportional to the liquid-crystal surface tension (σ), but inversely proportional to the length (L) between polymer strands; C is a constant. If the amount of polymer adsorption increases, the distance L between the polymer strands decrease, resulting in an increased subcooling ΔT performance. Conversely, if the amount of inhibitor adsorption decreases (due to depletion by multiple small hydrate crystals) the distance L between polymer strands increases, resulting in a smaller subcooling ΔT.

Initial field tests of kinetic inhibitors were reported by ARCO (Bloys et al., 1995) and Texaco (Notz et al., 1995). Bloys reported the effectiveness of 0.3–0.4 wt% VC-713 in a 17-day test in a North Sea pipeline. Other large field applications, include BP's West Sole/Hyde 69 km wet gas pipeline where the maximum subcooling was 8°C (Argo et al., 1997; Philips 1997), the BP operated Eastern Trough Area Project (ETAP) in the British Sector of the North Sea (Philips 1997; Palermo et al., 2000) where the subcooling was 6–8°C. In the latter ETAP application, kinetic inhibitors replacing methanol were used. A similar method was used by Elf (now Total) to replace methanol in an onshore multiphase transportation line (Leporcher 1998; Kelland 2006). More recently, PVCap kinetic inhibitors have been applied in Qatar involving about 100–120 tn of PVCap per year, representing the largest applications of kinetic inhibitors in the world.

It should be noted here that, while PVP was one of the first kinetic inhibitors discovered, it is one of the weakest kinetic inhibitors available.

Examples of the use of modern kinetic inhibitors are given by Fu (2002) and Kelland (2006). Perhaps the best kinetic inhibitor copolymer was developed by ExxonMobil (Talley, Personal Communication, February 20, 2006) as the *N*-methyl-*N*-vinylacetamide: polyisopropyl-methacrylamide 1:1 low molecular weight copolymer (VIMA:IPMA 1:1) that can provide a subcooling of up to 22–23°C. However, the use of VIMA:IPMA is determined by availability and cost. Table 8.1 summarizes the development of kinetic inhibitors in chronological order, a qualitative ranking of these inhibitors is also given. Much of this historical development of kinetic inhibitors has been excerpted from the recent review of LDHIs by Kelland (2006).

In his review of LDHIs, Kelland shows that kinetic inhibitors are well-established tools for hydrate prevention, with the following three points:

1. Low molecular weight PVCap-based products with added synergists were the best kinetic inhibitors for structure II hydrates on the market in 2005, and these inhibitors can provide 48 h of inhibition at a subcooling of 13°C.
2. In 2005, 40–50 applications of kinetic inhibitors operated worldwide, with the largest applications in the North Sea and Qatar Applications.
3. In 2000 the sales of PVCap-based polymers were 300–500 tn per year.

8.2.3.1 Antiagglomerant means of preventing hydrate plugs

As shown in Figure 8.8, in oil-dominated systems there are three ways to prevent hydrate plug formation: (1) prevent particle nucleation, (2) prevent particle growth, and (3) prevent agglomeration of particles so that plugs will not form. AAs prevent the latter aggregation stages that lead to plugging.

AAs are surface active agents that reduce particle adhesion. The AA method was begun by Behar, Sugier, and coworkers at l'Institut Francais du Petrole in 1987 (Behar et al., 1988). Chemicals effective as AAs are surfactants that typically provide a relatively stable water-in-oil emulsion. The developments by l'Institut Francais du Petrole were followed by Shell with surfactants of alkylarylsulfonic acid and its salts (Muijs et al., 1991) and alkyl glycocides (Reynhout et al., 1993). In Bishnoi's laboratory, Kalogerakis et al. (1993) showed that some surfactants increased the agglomeration tendency, counter to the desired effect. Many of these first chemicals, as well as surfactants and polymers were shown to be ineffective through testing by Urdahl et al. (1995).

Figure 8.12 shows the macroscopic method of AAs. In the top portion of the figure, hydrates are agglomerated into a plug, analogous to that in the far right of Figure 8.8. In the lower portion of the figure, the hydrate particles are dispersed in the hydrocarbon liquid, so that they will continue to flow.

There are two types of AAs: (1) the French Petroleum Institute (IFP) type that provides a special kind of water-in-oil emulsion so that on hydrate formation, the emulsion will not agglomerate and (2) the Shell type that have hydrate-philic head group(s) and long hydrophobic tail(s). Because the IFP-type of AA still awaits a

TABLE 8.1
Chronology of Kinetic Inhibitor Developments

Kinetic hydrate inhibitor (KHI)

Brief name	Chemical name	Research group (reference)	ΔT sub (°C)
PVP	Poly-*N*-vinylpyrrolidone	CSM (Long et al., 1994)	5
HEC	Hydroxyethylcellulose	CSM (Long et al., 1994)	
PVCap	Poly-*N*-vinylcaprolactam	CSM (Long et al., 1994)	8–9
Graffix VC-713	Terpolymer of vinycaprolactam (VCap), vinylpyrrollidone (VP), and dimethlyaminoethyl methacrylate	CSM (Sloan, 1995a,b)	8–9
Polyelectrolytes		CSM (Sloan, 1995a,b)	
Polyether block copolymers		CSM (Sloan, 1995a,b)	
Polyvinylamides	For example, poly(*N*-methyl-*N*-vinyl acetamide)	CSM (Sloan, 1995a,b)	
Polyalkylacrylamides	For example, polyethylacrylamide	CSM (Sloan, 1995a,b)	
Polyalkyloxazolines	For example, polyethyloxazoline	CSM (Sloan, 1995a,b)	
AFPs	Antifreeze proteins (from winter flounder)	BP/Shell (Edwards, 1994)	
AGGPs	Antifreeze glycoproteins (from winter flounder)	BP/Shell (Edwards, 1994)	
Butylated PVP	Butylated poly-*N*-vinylpyrrolidone	Shell (Anselme et al., 1993)	
Amino acids	Tyrosines and related chemicals	BP (Duncan et al., 1993)	
Threshold inhibitor blends	For example, polyvinylcaprolactam + tetrabutylammonium bromide, or + tetrapentylammonium bromide	BP (Duncan et al., 1996)	<10
Polyamino acids	Poly-L-proline (related to fish antifreeze protein)	RF (Rogaland Research)	
VIMA:VCap 1:1	*N*-methyl-*N*-vinylacetamide:vinylcaprolactam 1:1 copolymer	RF/Exxon (Colle et al., 1996, 1999)	10–11
VCap:vinyl imidazole		RF	

(Continued)

TABLE 8.1
Continued

Kinetic hydrate inhibitor (KHI)

Brief name	Chemical name	Research group (reference)	ΔT sub (°C)
Ring-opened polyethyloxazoline	Contains ethylamide groups in repeating unit of polyethyloxazoline	RF	
Polymer-containing amide groups	For example, polyalkylacrylamides, polydialkylacrylamides, polyvinylamides, polyallylamides, polymaleimides, polymers of cycliciminoethers and polyalkyloxazolines, and amides and esters of N-acyldehydroalannine	Exxon (Colle et al., 1996)	
PolyAP and Poly-iPAm	Acrylamide polymers—polyacryloylpyrrolidene (polyAP) best, followed by polydiethylacrylamide, then polyisopropylacrylamide (poly-iPAm)	Exxon (Colle et al., 1996)	
PolyVIMA	Poly-N-methyl-N-vinylacetamide	Exxon (Colle et al., 1996)	
Copolymers of VIMA with other alkylamide polymers	For example, 1:1 VIMA:iPMA (isopropylmethacrylamide) copolymer gave 4°C higher subcooling than polyiPMAM	Exxon (Talley and Oelfke, 1997)	∼13.5
Ring-closed oxazaline polymers		Exxon	
VIMA:vinyl butyrate copolymer		Exxon	
Alkyl acrylate:VP copolymers	For example, butyl acrylate:vinyl pyrrolidone copolymers	RF/Nippon Shokubai (NS) (Namba et al., 1996)	
Surfactants as synergists with KHI polymers	For example, butyl sulfate, sodium valerate, zwitterionics, such as butyldimethylammonium butylene sulfonate, and N-dodecylpyrrolidone	Exxon (Colle et al., 1996)	
KHI blends of TBAB and VCap polymers		BP/Clariant	10
Small alcohols and glycol ethers (3–5 C's) as synergists for VC polymers	For example, butyl glycol ether (BGE) synergist (and solvent) of PVCap	ISP	
Modified AMPS polymers with 5-carbon tail	Modified acrylamidopropylsulfonic acid polymers; homopolymer of monomer	Exxon (Pfeiffer et al., 1999)	
Modified AMPS monomer with VCap	Copolymers of modified acrylamidopropylsulfonic acid monomer with vinylcaprolactam	Exxon (Pfeiffer et al., 1999)	

Acrylamide:AMPS copolymers		IFP (Sinquin et al., 1998)	
Polymers with at least one N containing monomer	Dimethylaminomethylacrylate monomer	IFP (Sinquin et al., 1998)	
AP:VCap copolymer		RF	
Synergistic 2:1 blend of 90/10 iPA/AMPS:PVCap		NS/RF (Kelland et al., 2000)	12
TBAO and TPAO with PVCap	Tributylamine oxides and tripentylamine oxides	Clariant (Klug et al., 1998)	
VIMA: IPMA 1:1 low MWt copolymer (oligomer)		Exxon (Talley and Oelfke, 1997)	11
PVCap oligomer		CSM	
PVCap oligomer	MWt 1500 gave best activity	ISP/BP (Bakeev et al., 2000, 2001, 2002)	
Copolymers of VCap	Containing small amounts of comonomer: dimethylaminoethylacrylate or N-(3-dimethylaminopropyl)methacrylamide	ISP (Thieu et al., 2002)	
VCap:vinyl pyridine copolymers		ISP (Bakeev et al., 2001)	
Polyoxyalkylenediamines as synergists for VCap polymers		ISP (Bakeev et al., 2000)/BJ Unichem	
Hybranes	Hyper-branched polyesteramides	Shell (Klomp, 2001)	
Polyesteramide KHIs with PVCap as synergist	Typical polyesteramide made from di-2-propanolamine, hexahydrophthalic anhydride and bis-(dimethylaminopropyl)imine. Synergists: polyethyleneimine reacted with formaldehyde and caprolactam giving polymers with pendant caprolactam rings; N-methyl butylamine reacted with formaldehyde and polyacrylamide	Baker Petrolite (Rivers and Crosby, 2004)	
Amidated maleic anhydride copolymers with ether carboxamine surfactant synergists		Clariant	
PVCap (low MW) with synergists		ISP/Nalco (Fu et al., 2002)	
Low MW lactam-based polymer		BASF (Neubecker, 2006)	
Water-soluble vinyl lactam copolymers	For example, 80:20 VP:butyl acrylate	BASF (Angel et al., 2004, 2005)	

(Continued)

TABLE 8.1
Continued

<div align="center">

Kinetic hydrate inhibitor (KHI)

</div>

Brief name	Chemical name	Research group (reference)	ΔT sub (°C)
VCap:alkyl(methyl)acrylate ester copolymers	Copolymers contain short-chain alkyl methacrylates, such as methyl methacrylate	Clariant (Dahlmann et al., 2004)	
PEO (high MW) as synergist for PVCap	Poly(ethylene oxide)	Lee and Englezos, (2005)	
PolyIPMA	Poly isopropylmethacrylamide	Exxon/Mitsubishi (Toyama and Seye, 2002)/ISP (Thieu, 2002)	
Polymers with bimodal MWt distribution	Synthesized from single polymerization or by mixing two polymers with unequal MWt distributions. Polymer is polyIPMA, as well as PVCap and other polymers	ExxonMobil (Colle et al., 2005)	24
Polymeric emulsifier mixed with nonionic nonpolymeric coemulsifier			12
Polyalkoxylated amines	Alkoxylation with, for example, propylene oxide (PO). Preferred amine is triethanolamine, or ammonia and other alkanolamines used; amine can also be quaternized; Best example is triethanol with 14.9 PO units	Akzo Nobel (Burgazli et al., 2003)	
Derivatives of poly(vinyl alcohol) by reaction with aldehydes	Contains vinyl ester acetal functionalities besides some unreacted vinyl alcohol monomer units. Preferred aldehyde is butyraldehyde	Kurarau Specialties Europe (Dahlman et al., 2004)	
Grafted polymers	Backbone, for example, polyalkylene glycol, polyalkyl-eneimine, polyether, or polyurethane, and active functional side groups made from grafting VP or VCap to backbone using radical initiators	BASF (Maximilion et al., 2005)	
Polyquaternaries with pendant TBA groups	TBA (tributylammonium groups)	RF/Stavanger U (Kelland, 2006)	

Without antiagglomerant
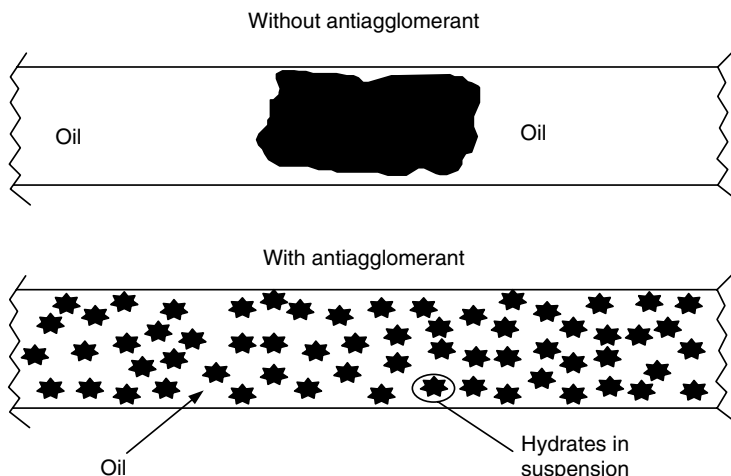

With antiagglomerant

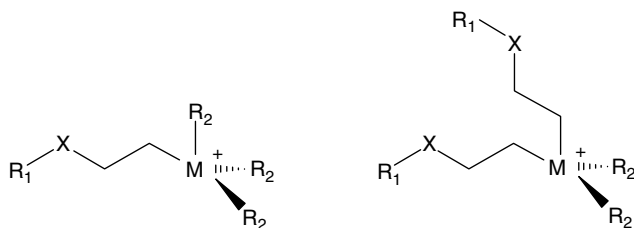**FIGURE 8.12** The macroscopic mechanism of hydrate antiagglomerant slurries.

FIGURE 8.13 The two Shell-types of antiagglomerant. On the left is the water-soluble type, with one branch (R_1) containing 8–18 carbons. On the right is the oil-soluble type with two branches (R_1) with 8–18 carbons. The central atom is nitrogen or phosphorus, and the shorter branches (R_2) are butyl- or pentyl-groups.

field trial (Kelland, 2006) we will concentrate here on the Shell-type AA, which can be further categorized as (1) water soluble, with one long hydrocarbon tail or (2) oil soluble, with two long hydrocarbon tails. Both of these types are shown in Figure 8.13.

A typical water soluble Shell-type AA is a quaternary ammonium salt (QAS), in which two or three of the four ammonium branches are short (e.g., a butyl compound that might be a candidate for inclusion within hydrate cavities) and one or two branch(es) are much longer (e.g., C8 to C18) so that it might be soluble within the oil phase. The mechanism of AAs is uncertain at this time, but some educated guesses can be given, which evolve from the chemical structure of AAs.

The butyl-ammonium end of the AA is very attractive to water and to hydrates, so that it remains firmly attached either to the water droplet, or to the hydrate phase after the water droplet conversion. The other, long carbon end of the AA has the

function of stabilizing the QAS in the liquid hydrocarbon, using the physical chemistry principle of "like dissolves like." So the attachment of one end of the AA to the hydrate with the other end dissolved in the hydrocarbon liquid turns the spherical hydrate shells in Figure 8.8 to spheres with protruding strands of chemicals.

These long protruding chemical strands provide separation of the hydrate particles, so that agglomeration does not occur for the suspension in the oil phase. As measured by Yang et al. (2004) and by Taylor (2006), without such prevention the capillary forces between the hydrate particles are very strong, and can lead to large hydrate masses.

In antiagglomeration, since the prevention method relies on emulsified water/hydrates, a condensed hydrocarbon is required (Mehta et al., 2003). The solid phase loading cannot exceed 50 volume% of the liquid hydrocarbon phase to prevent high viscosity associated with compacted slurry flow. The emulsion is broken and water is removed onshore or at a platform.

The oil-soluble Shell-type AA may behave similarly, but with two long-chain hydrocarbon tails to maintain solubility in the oil phase. However, of the two categories of Shell-type AAs, the water-soluble type has had the widest use. With the above broad-brush, conceptual picture of AAs, it is clear that further definition should be done for refinement of the AA mechanism.

8.2.4 Case Study 6: AAs are a Major Hydrate Plug Prevention Tool

Mehta et al. (2003) review the shortcomings of traditional thermodynamic inhibitors, and the use of the new LDHIs, which are based upon kinetic principles, and are typically applied in concentrations less than 1 wt%. They note that the new KHIs have an upper subcooling limitation of approximately 20°F, while deepwater developments often have subcooling requirements of 35–40°F.

In addition, Mehta et al. present a case study of Shell's Popeye field use of a new AA inhibitor in a gas condensate line, with the following points:

1. The AA works by emulsifying hydrates in the hydrocarbon liquid. Hydrates are carried as a nonagglomerated slurry, without viscosity increase for up to 50% water cuts.
2. The AA limit to water cut (volume of water per volume of oil) is approximately 60%.
3. In the field case study, the AA effectively inhibited hydrate formation, with no significant downstream problems.
4. Flowlines are continuously treated with AA before shut-in, eliminating the need for instantaneous corrective actions (e.g., flowline depressurization) on shut-in.
5. The volume reduction of injected inhibitor can be reduced by a factor of 25 relative to methanol, allowing less topside storage space, easier transportation, and smaller umbilicals.

6. The AA eliminates methanol discharge in overboard water and export lines.
7. CAPEX savings are particularly appealing with the use of AAs for new projects, but OPEX savings may justify retrofits of existing projects.

Table 8.2 summarizes the chronological development of AAs. As of April 1, 2004, AAs were used in 17 gas and oil fields in the Gulf of Mexico, with prospects for rapid expansion. However, as of this writing, kinetic inhibitors are predominantly used in LDHI work.

8.3 How is a Hydrate Plug Dissociated?

This section provides a qualitative understanding of CSMPlug, the plug dissociation program which accompanies this book and is illustrated in Appendix B. Sometimes a hydrate plug does form, with the consequences of blocking fluid flow. When a flowline plugs, the usual responses are

1. Locate the plug to determine its position and length
2. Carefully evaluate the safety concerns of plug removal (please read the following section to determine the major safety implications imposed by hydrate plugs)
3. Evaluate the methods of plug removal, of which there are four types:
    a. Hydraulic methods such as depressurization
    b. Chemical methods such as injection of inhibitors or reactive chemicals that generate heat (Freitas et al., 2002)
    c. Thermal methods that involve direct electrical heating (Davies et al., 2006)
    d. Mechanical methods with coiled tubing, drilling, etc.

The below concepts are an extension of those in Chapter 3 of *Hydrate Engineering* (Sloan, 2000). Details of the model can be found in the work by Davies et al. (2006). Here, only the first, most-common method of depressurization is treated conceptually.

From both a safety and technical standpoint, the preferred method to dissociate hydrate plugs is to depressurize from both sides. Depressurization is particularly difficult when the liquid head on the hydrate plug is greater than the dissociation pressure, as in mountainous terrain or in very deepwater, in which case electrical heating may be used (Davies et al., 2006), a method not considered here.

When a hydrate plug occurs in a pipeline at temperatures above the ice point, the pressure–temperature conditions are illustrated in Figure 8.14. To the left of the three phase (L_W–H–V) line hydrates can form, while to the right only fluids can exist. Because the lowest ground burial temperatures or ocean temperatures (39°F) are usually above 32°F, ice formation (which will also block flows) is not a normal

TABLE 8.2

Chronology of Antiagglomerant Developments

AA inhibitors

Brief name	Chemical name	Research group (reference)
IFP dispersant additives	Diethanolamides	IFP (Sugier et al., 1989)
IFP dispersant additives	Dioctylsulfosuccinates	IFP (Sugier et al., 1989)
IFP dispersant additives	Sorbitans	IFP (Sugier et al., 1989)
IFP dispersant additives	Ethoxylated polyols	IFP (Sugier et al., 1989)
IFP dispersant additives	Ethoxylated amines	IFP (Sugier et al., 1989)
Polymeric surfactants	Based on polyalkenyl succinic anhydride	IFP (Sugier et al., 1989)
Alkylarylsulfonates	Surfactant	Shell (Muijs et al., 1991)
Alkyl glucosides	Surfactant	Shell (Reynhout et al., 1993)
TBAB, a QAS	Tetrabutylammonium bromide-quaternary ammonium surfactants	Shell (Klomp et al., 1995)
TPAB, a QAS	Tetrapentylammonium bromide-quaternary ammonium surfactants	Shell (Klomp et al., 1995)
Water soluble single-tail QAS	For example, tributylammonium or tripentylammonium (better) headgroup	Shell US
QAS	Quaternary ammonium surfactants - ≥ 2 n-butyl, n-pentyl, isopentyl groups	Shell (Klomp et al., 1995)
QAS	Replacing 1 or 2 small alkyl groups with long hydrophobic tail (8–18 carbon atoms)	Shell (Klomp et al., 1995)
Polyalkoxylates	Polypropoxylates	RF
Polyalkoxylate amine	Polyalkoxylate amine, MW 6000	Akzo Nobel
Planteren 600 CPUS	An alkyl glucoside	RF
Polymeric emulsifiers	Polyglycol derivatives of polyalkyenylsuccinic anhydride	IFP (Behar, 1994)
Twin-tailed QAS	Tetraalkylammonium salts with two tails, such as dicocoyldibutylammonium bromide	Shell/Akzo Nobel (Klomp and Reijnhart, 1996)
Twin-tailed QAS	Diesters of dibutyldiethanolammonium halides and 2 mol alkyl carboxylic acid (optimum 12–14 carbons)	Shell/Akzo Nobel (Klomp and Reijnhart, 1996)
Polymeric surfactants, for example, Emulfip 102b	50% solution of polymerized fatty acids and amides in rapeseed oil	IFP/EUCHARIS (Palermo et al., 1997)

|		
Polyetherpolyamine and polyetherdiamines	Polyetherpolyamines and polyetherdiamines (particularly of the oxypropylene type)	BJ Unichem (Pakulski, 1998, 2001)
Polyetherpolyamine	Quaternized polyetherpolyamines reacted with a long-chain alkyl bromide	BJ Unichem (Pakulski, 2001)
Span sorbitan surfactant		CSM (Huo et al., 2001)
Monotail surfactants with caprolactam headgroup and polymeric surfactants based on VC oligomer or *N*,*N*-dialkylacrylamides with alkyl thioether end groups	Dodecyl-2-(2-caprolactamyl) ethanamide	CSM (Huo et al., 2001)
Oil soluble twin-tailed QAS	*N*-butyl diethanolamine and methyl or ethyl branch added to ethylene spacer groups between ester groups and quaternary N atom	Shell (Klomp, 1999)
Monomeric surfactants with alkylamide or dialkylamide groups in head	For example, groups mostly carbonylpyrollidone and isopropylamide goups performed well in KHI polymers	RF/NS (Kelland, 2000)
Hybranes	Hyper-branched polyesteramides	Shell (Klomp, 2001)
VCap:alkyl(methyl)acrylate ester copolymers	Copolymers contain long-chain alkyl methacrylates, such as oleyl methacrylate	Clariant (Dahlmann, 2004)
Water-soluble quaternary AA (onium compound)	Formulated with amine salt containing alkyl or hydroxylalkyl groups (1–3 carbons) or ammonium salt, and optionally a solvent	Baker Petrolite (Przbylinski and Rivers, 2003)
QAS phase separation		Shell (Blytas and Kruka, 2001)
QAS detoxified	Addition of anionic polymers or anionic surfactants	Baker Petrolite (Rivers et al., 2004)
Ion pair mixture	QAS + anionic, nonionic, or amphoteric compound, for example, dodecylbenzenesulfonic acid (DDBSA) + quaternary ammonium compound (with appendages <6 carbons)	Baker Petrolite (Crosby et al., 2005)
Hydrophobic oil-soluble block copolymers	Emulsion AA (Emulfip 102b, IPE202b), for example, made from polyalkenylsuccinic anhydride with monoether of poly(ethylene glycol); typical block copolymer is made from styrene/ethylene/propylene	IFP (Gateau et al., 2004)
QAS	Quaternary center with butyl or pentyl groups	Nalco (Cowie et al., 2003)
QAS	QAS with ether spacer group between quaternary N atom and long alkyl tail	Goldschmidt (Milburn and Sitz, 2002)
QAS	Alkylaminoalkyl mono- and diesters; *N*,*N*′-dialkylaminoalkylether carboxylates; alkylaminoalkyl/alkoxy monoesters	Clariant (Dahlmann, 2004)
Amine oxides and betaine surfactants		Champion Tech. (Panchalingham et al., 2005a,b,c,d,e)
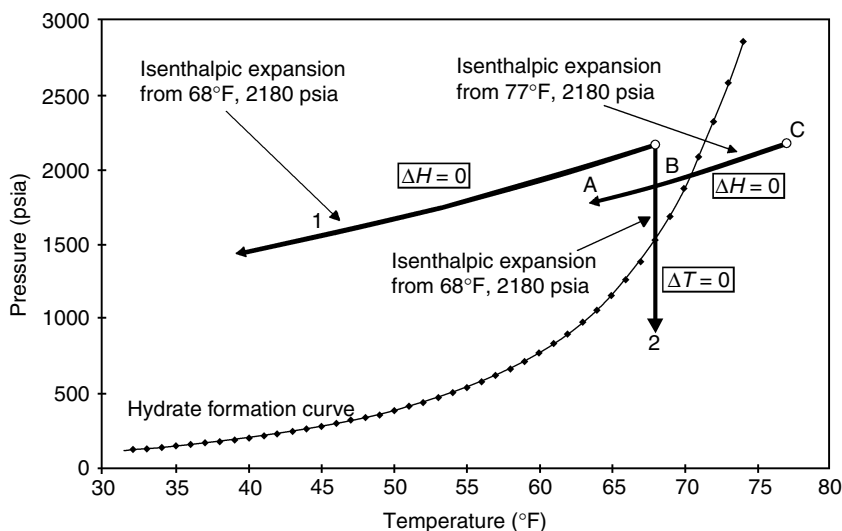
FIGURE 8.14 Temperature changes as a result of depressurization (1) isenthalpic rapid expansion as through a valve, and (2) very slow depressurization, as in a large-volume pipeline. Note that for the rightmost case, a fluid system can be expanded into the hydrate region, as calculated by the methods in Section 4.2.1.1 and the programs of CSMGem on the CD accompanying this book.

operating concern. When hydrates form, flow is blocked so that the plug temperature rapidly decreases to the surroundings temperature at the pipeline pressure. Figure 8.14 shows the rapid depressurization of a pipeline hydrate plug to Point A causes it to proceed further into the two-phase (H–V) region, with an excess gas phase, so that the liquid water has converted to hydrate.

When a hydrate plug occurs in a pipeline at temperatures above the ice point, the three conditions (sufficient temperature, pressure, and composition) exist for hydrate formation. When hydrates form, flow is blocked so that the plug temperature rapidly decreases to the surroundings temperature at the pipeline pressure.

Pressure reduction is accompanied at the hydrate interface by a temperature decrease to the equilibrium temperature. Normally the pipeline cannot be depressured sufficiently rapidly for Joule–Thomson (isenthalpic) cooling to lower the temperature; this would occur through a restriction such as a valve. If the pressure is reduced slowly, a vertical isothermal depressurization ($\Delta T = 0$) results. Usually an intermediate pressure reduction rate causes the hydrate interfacial temperature to be significantly less than the surroundings, causing heat influx from the surroundings to melt hydrates from the pipe boundary inward.

With rapid extreme pressure reduction, the hydrate equilibrium temperature can decrease below 32°F for a methane hydrate depressurized to atmospheric

pressure. In this case the water from the dissociated hydrate buffers the temperature reduction to around 0°C, by converting to ice below the solid–liquid line. If ice formation occurs with hydrate dissociation, then the question arises, "How will the ice plug dissociation rate compare to the hydrate dissociation rate in an ocean pipeline?"

Recent experiments and modeling suggests that blockages are most efficiently removed when the line is depressurized to the fullest extent, as rapidly as possible. When ice forms, it normally has a lower temperature and higher thermal diffusivity than hydrates, resulting in a rate increase of heat transfer into the pipe.

During 1994–1997 field studies, over 20 hydrate plugs were systematically formed and removed from a 6 in. North Sea line in the Tommeliten Gamma field. In both laboratory and field studies these plugs were found to be very porous (>50%) and permeable. Porous, permeable hydrates easily transmit gas pressure while still acting to prevent liquid flow in the pipeline. When the pressure was decreased at both ends of a highly porous hydrate plug, the pressure decreased throughout the entire plug to a constant value. The dissociation temperature at the hydrate front is determined by the pipeline pressure and by the buffering capacity of the water fusion to ice.

Pipeline depressurization reduces the hydrate temperature below the temperature of the surroundings. Heat flows radially into the pipe, causing dissociation first at the pipe wall as shown in Figure 8.15. In the figure three laboratory hydrate plugs are shown after three separate experiments—after 1, 2, and 3 h of dissociation (Peters, 1999). Radial hydrate dissociation controls plug removal, because the pipe diameter (typically less than 2 ft) is at least an order of magnitude less than the length of a hydrate plug (frequently more than 50 ft) in a pipeline.
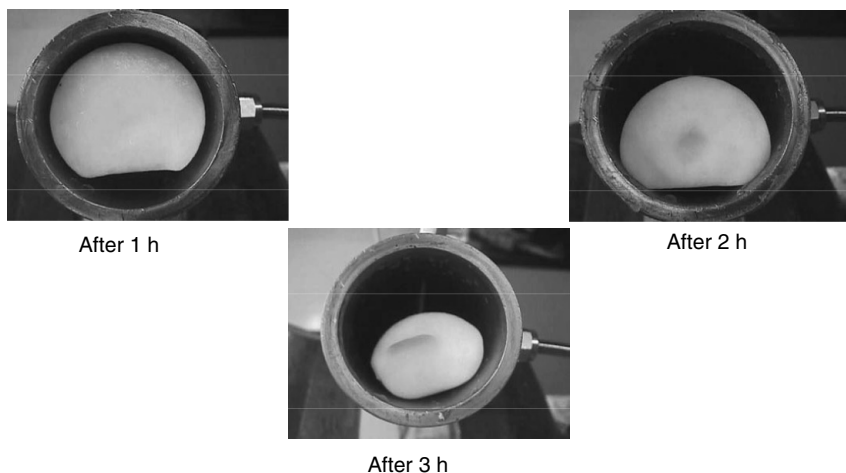
Pictures of dissociating hydrate plugs

After 1 h

After 2 h

After 3 h

FIGURE 8.15 Hydrate plug radial dissociation in three experiments.

The radial dissociation concept is in contrast to previous longitudinal dissociation concepts of nonporous hydrates, in which depressurization from both ends was supposed to result in dissociation progressing from the plug ends toward the middle (Yousif et al., 1990). As shown in Figure 8.15 when the temperature of the hydrate is lower than that of the surroundings, heat flows radially into the plug, causing dissociation along the entire length. Of course, some plug dissociation occurs at the ends, but due to much smaller dimensions, the radial dissociation (which occurs simultaneously along the plug length) controls blockage removal.

A close inspection of the first photo (1 h) in Figure 8.15 shows the periphery of the first plug has a different morphology than its inner section. This is because, when hydrates dissociate, the energy is drawn from the phase with the highest thermal diffusivity—the water phase from the melted hydrate. That is, the hydrate converts to a peripheral ice plug, and the ice plug subsequently converts to water. The problem of hydrate plug dissociation is two moving boundaries, the inner, hydrate + ice boundary, and the outer, ice + water boundary. The water has a higher thermal diffusivity than gas and caused the flat spot at the bottom of the plugs in Figure 8.15. However, water cannot be seen in the figure, because it flowed out of the horizontal pipe, once it was opened to the atmosphere in each of the three photos.

Because hydrate plug detachment occurs first at the pipe wall, a partially dissociated plug will move down the pipeline when the line is restarted with a pressure gradient, only to result in a later plug at a pipeline bend, depression, or other obstruction. The second plug blockage can be more compact than the first, for example, if there is substantial momentum on impact at the bend. In extreme cases the plug can act as a projectile, which may result in severe safety problems as indicated in the following section. As a result, methanol is used to dissociate the plug, when the annulus is sufficient to allow flow around the plug.

The concepts are similar for both onshore and subsea pipelines. In the above conceptual picture, it is assumed that the pipeline wall temperature is constant at 39°F. If a line is insulated, hydrate dissociation becomes much more difficult because the insulation that prevented heat loss from the pipe in normal operation will prevent heat influx to the pipe for hydrate dissociation. Alternatively, if the pipe is buried, the pipe wall temperature will be greater than 39°F and the system may be insulated by the ground.

Austvik et al. (1997) noted some exceptions to radial dissociation, particularly for plugs of low porosity/permeability or for very long plugs. As shown by Berge et al. (1998) hydrate plugs consolidate after plug formation, causing porosity and permeability to decrease considerably. The amount of water converted to hydrate is very low, often as low as 2–4%, due to the thin hydrate films shown in Figure 8.8. Hydrate plugs should be dissociated as soon as possible to take advantage of higher porosity, permeability, and lower fractions of hydrate.

Hydrate depressurization. Hydrate depressurization must always be done very carefully. The two methods of dissociation are from both sides of the plug(s),

or from one side of a plug(s). There are two reasons for the preferred method of two-sided hydrate plug dissociation:

1. For a single plug, dissociation from both sides eliminates the safety concern of having a projectile in the pipeline. As indicated in the next section this is a major safety concern. Sometimes plug dissociation can cause projectiles that damage equipment and in the extreme, can cause a loss of life. It should be noted, however, that sometimes gas trapped between two plugs can cause risks, even for two-sided dissociation, as indicated in Section 8.4 on Safety.
2. Two-sided dissociation eliminates the Joule–Thomson cooling that may stabilize the downstream end of the plug. With radial dissociation along the plug, two-sided dissociation is more than twice as fast as single-sided dissociation.

For the above reasons, the upstream portion of a hydrate plug should be dissociated through a second production line, if available. If this is impossible, depressurization through an umbilical for injecting inhibitors at the wellhead may be possible; in this case provision should be made for removing or bypassing any check valve that may be in the service line at the wellhead. In extreme cases, where the line cannot be depressurized due to a high liquid head on the plug, it may be possible to use electrical heating to dissociate the plug, as indicated by Davies et al. (2006) and as practiced on the Nakika gas field operated by BP, but designed by Shell.

Two-sided dissociation is almost always the method of choice for the flow assurance engineer. Many of the concerns with single-sided plug dissociation are discussed by Davies et al. (2006). The program CSMPlug and a User's Manual are provided on the CD in the endpapers of this book. Appendix B contains a set of User's examples to enable the engineer: (1) to estimate the time for two-sided dissociation, (2) to estimate the time required for (very careful) single-sided dissociation, and (3) to estimate the safety concerns of the hydrate, such as velocity and plug displacement.

8.3.1 Case Study 7: Gulf of Mexico Plug Removal in Gas Export Line

A hydrate blockage in the export line from Shell's Bullwinkle platform in the Green Canyon Block 65 to the Boxe platform was reported in DeepStar Report A208-1 (Mentor Subsea, 1996, p. 52). The 12 in., 39,000 ft line was not insulated. The seawater temperature was 50°F at the base of the platform in 1,400 ft of water. Gas gravity was 0.7 and the flow rate was 140 MMscf/d at an inlet pressure of 800 psi.

Gas hydrates formed during a restart after the platform was shut down due to a hurricane. During the shut-in period the gas dehydrator partially filled with water. After production restarted, since the dehydrator was not cleaned properly, it was not dehydrating gas as designed and wet gas entered the export line, causing

water condensation and hydrate formation. A complete hydrate blockage formed in less than 1 h, just past the base of the export riser at a low spot.

To remove the blockage, the line was depressured on both sides of the plug. Then methanol was circulated into the line to accelerate the hydrate dissociation rate. After complete removal of the hydrates, the dehydrator was cleaned, inspected and restarted properly. The entire remedial operation required 36 h to complete. The major cost was the lost production time.

8.4 SAFETY AND HYDRATE PLUG REMOVAL

There are many examples of line rupture, sometimes accompanied by loss of life, attributed to the formation of hydrate plugs. Hydrate safety problems are caused by three characteristics:

1. Hydrate density is similar to ice, and upstream pressure can propel a dislodged hydrate plug at high velocity. In 1997 DeepStar Wyoming field tests, plugs ranged from 25 to 200 ft with velocities between 60 and 270 ft/s. Such velocities and masses provide sufficient momentum to cause two types of failure at a pipeline restriction (orifice), obstruction (flange or valve), or sharp change in direction (bend, elbow, or tee) as shown in Figure 8.16. First, hydrate impact can fracture the pipe, and second, extreme plug momentum and gas compression can cause pipe rupture downstream of the hydrate path.
2. Hydrates can form either single or multiple plugs, with no method to predict that will occur. High differential pressures can be trapped between plugs, even when the discharge end of plugs are depressurized.
3. Hydrates contain 164 volumes (STP) of gas per volume of hydrate. When hydrate plugs are dissociated by heating, any confinement causes rapid
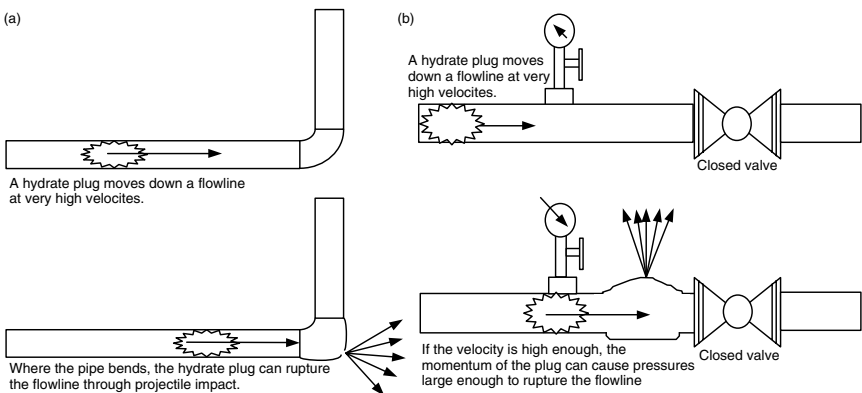

FIGURE 8.16 Two ways a plug can rupture a pipe: (at left) via momentum impact of high velocity projectile at a pipeline bend, and (at right) via a combination of plug momentum and gas compression at a pipeline obstruction.

gas pressure increases. However, heating is not an option within buried pipe due to the difficulty of plug location and economics of heating an inaccessible pipeline.

When a plug is depressured using a high differential pressure, the dislodged plug can be a very dangerous projectile, as the below case study indicates (from Mobil's Kent and Coolen, 1992).

The first chapter of Sloan (2000) is devoted to hydrate safety principles, showing several types of safety problems associated with a hydrate plug. Here only one precautionary example is given.

8.4.1 Case Study 8: Hydrate Plug Incident Resulting in Loss of Life

At a major energy company in Alberta, a foreman and operator were attempting to clear a hydrate plug in an outlying sour gas flowline. They had bled down the pressure in the distant end from the wellhead. They were standing near the line when the line failed, probably from the impact of a moving hydrate mass. A large piece of pipe struck the foreman and the operator summoned help. An air ambulance was deployed; however, the foreman was declared dead on arrival at the hospital. No preexisting pipe defects were found.

The *Canadian Association of Petroleum Producers Hydrate Guidelines* (King et al., 1994) suggest three safety concerns in dealing with hydrate blockages:

- Always assume multiple hydrate plugs; there may be pressure between the plugs.
- Attempting to move ice (hydrate) plugs can rupture pipes and vessels.
- While heating a plug is not normally an option for a buried pipeline, any heating should always be done from the end of a plug to release the gas, rather than heating the plug middle.

The above case study warns that hydrates can be hazardous to personnel and to equipment. Yet hydrate plugs can be safely dissociated with the use of CSMPlug and User's Manual on the CD in the endpapers of this book, with the User's Guide Examples in Appendix B. The safety option of this program and process should be considered first, so that the potential for overpressurization and eruption can be considered.

In ocean drilling, hydrated sediment cores are often obtained. Because the cores frequently traverse warm waters for periods of about 1 h, hydrated cores dissociate and release gas, to yield higher pressures. When core liners are retrieved on the deck of a drilling vessel, frequently the warm weather can cause additional hydrate dissolution, resulting in further pressure increases. The modeling of this dissociation has been done by Wright et al. (2005) and by Davies et al. (2006).

To counteract these shipboard safety problems, several steps are taken such as drilling through core liners to relieve the pressure, or placing wooden barriers at

Core liner failure at APC/XCB transition

FIGURE 8.17   Core liner failures due to hydrate gas release on ship board.

the open end of cores. Nevertheless, with these cautions, exploding core liners can occur, as shown by Figure 8.17. These examples point to the need for a hydrate core safety manual, whose basis is in experiment.

8.5 APPLICATIONS TO GAS TRANSPORT AND STORAGE

It is estimated that about 70% of the total gas reserve is either too far from an existing pipeline or too small to justify a liquefaction facility. Gudmundsson and Borrehaug (1996, 2000) suggested that it is economically feasible to transport stranded gas in hydrated form. In the fourth international hydrate conference Mitsui Shipbuilding (Nakajima et al., 2002) show that work in conjunction with the Japan Maritime Research Institute (Shirota et al., 2002) provides a basis for extending the basic concept by Gudmundsson and Borrehaug to ship stranded gas.

For storage and transportation the self-preservation phenomenon of Section 3.3.3 could be an important phenomenon due to its requirements of decreased amounts of refrigeration. Recall that the self-preservation phenomenon was described as: "Self-preservation" consists of a short rapid dissociation phase with a release of 5–20 vol% of the total methane in the hydrate sample. During this gas release, adiabatic cooling of methane as well as general heat absorption occur, resulting in a drop in temperature of between 3 and 7 K relative to the temperature of the external cooling bath. After this rapid dissociation phase, the methane hydrate remains "metastably preserved for up to 24 h." It is thought that

this phenomena is associated with an ice coating that prevents rapid dissociation, aided by ice defect propagation (Kuhs et al, 2004).

Frequently, hydrates become important in natural gas storage in salt caverns for peak shaving, or seasonal or diurnal volume averaging delivery of gases. The work by deRoo et al. (1983) discusses this process, regarding hydrate formation in high salt concentration, with their data provided in Chapter 6 on methane hydrate inhibited by sodium chloride.

8.6 Summary of Hydrates in Flow Assurance and Transportation

As the energy industry produces from more hostile environments, such as the ultra-deepwater and the arctic, flow assurance problems will increase. Associated higher pressures, colder temperatures, and higher concentrations of acid gases will cause hydrates to be a larger concern, frequently impacted economically by the high cost of thermodynamic inhibitors at high concentration, so that LDHIs will be more commonly used.

The industrial flow assurance paradigm is shifting from avoidance, enabled by thermodynamic inhibition, to risk management, enabled by application of kinetics. Examples of time-dependent flow assurance phenomena are kinetic inhibitors, AAs, plug dissociation, and electrical heating of pipelines for plug dissociation. Research support will move from thermodynamics, which is currently acceptably accurate for engineering applications, to time-dependent kinetics.

The current chapter shows the application of mainly thermodynamic calculations, which have their basis in Chapters 4 and 5. However, as indicated in Chapter 3, a fundamental kinetic model, separated from heat and mass transfer phenomena, has yet to be established, particularly at high concentrations to extend the measurements pioneered in the laboratory of Bishnoi during the last three decades. The generation of such a time-dependent growth model and its application is one of the major remaining hydrate challenges.

References

Angel, M., Neubecker, K., Stein, S., WO Patent Application 04/042190 (2004).

Angel, M., Stein, S., Neubecker, K., US Patent 6878788 (2005).

Anselme, M.J., Reijnhout, M.J., Klomp, U.C., WO Patent Application 93/25798 (1993).

Argo, C.B., Blaine, R.A., Osborne, C.G, Priestly, I.C., in *Proc. SPE International Symposium on Oilfield Chemistry*, SPE 37255 Houston, TX, February (2007).

Austvik, T., Hustvedt, E., Gjertsen, L.H., Urdahl, O., in *Proc. 75th GPA Annual Convention*, p. 205 (1997).

Bakeev, K., Chuang, J.-C., Drzewinski, M.A., Graham, D.E., US Patent 6117929 (2000).

Bakeev, K., Harris, K., Argo, C.B., Drzewinski, M.A., Graham, D.E., US Patent 6451892 (2002).

Bakeev, K., Myers, R., Chuang, J.-C., Winkler, T., Krauss, A., US Patent 6242518 (2001).

Behar, E., in *Gas Hydrate Seminar*, Trondheim, Norway, June (1994).

Behar, E., Sugier, A., Rojey A., "*Hydrate Formation and Inhibition in Multiphase Flow*," presented at BHRA Conference Operation consequences of Hydrate Formation and Inhibition Offshore, Cranfield, UK, November 3 (1988).

Berge, L.I., Gjertsen, L.H., Lysne, D., *Chem. Eng. Sci.*, **53**(9), 1631 (1998).

Bloys, B., Lacey, C., Lynch, P., in *Proc. 27th Annual OTC*, OTC 7772, Houston, TX, May 1–4 (1995).

Blytas, G.C., Kruka, V.R., International Patent Application WO 01/36895 (2001).

BP/Clariant, Internal unpublished reports, cited in Kelland, pp. 831, 834 (2006).

Brill, J.E., in *Flow Assurance as a Discipline*, *Flow Assurance 2003*, Galveston, Texas, September 23–25 (2003).

Burgazli, C.R., Navarrete, R.C., Mead, S.L., in *Proc. Canadian International Petroleum Conference*, Paper 2003-070, Calgary, Alberta, Canada, June 10–12 (2003).

Carroll, J.J., *Natural Gas Hydrates: A Guide for Engineers*, Gulf Professional Publishing, Houston, TX (2003).

Colle, K.S., Costello, C.A., Talley, L.D., Longo, J.M., Oelfke, R.H., Berluche, E., WO Patent Applications, 96/08672, 96/41784 and 96/41834 (1996).

Colle, K.S., Oelfke, R.H., Kelland, M.A., U.S. Patent Applications 58746560 (1999).

Colle, K.S., Talley, L.D., Longo, J.M., World Patent Application WO 2005/005567 (2005).

Cowie, L., Shero, W., Singleton, N., Byrne, N., Kauffman, L., *Deepwater Technology*, Gulf Publishing Co, p. 39 (2003).

Crosby, D.L., Rivers, G.T., Frostman, L.M., US Patent Application 2005/0261529 (2005).

Dahlmann, U., Feustel, M., Kayser, C., Morschchaeuser, R., US Patent Application 2004/00030206 (2004).

Davies, S.R., Selim, M.S., Sloan, E.D., Bollavaram, P., Peters, D.J., Hydrate Plug Dissociation, *AIChE J.*, **52**(12), 4016–4027 (2006).

de Roo, J.L., Peters, C.J., Lichtenthaler, R.N., Diepen, G.A.M., *AIChE J.*, **29**, 651 (1983).

Duncan, S., Edwards, A.R., Osborne, C.G., European Patent Application 0536950 A1 (1993).

Duncan, S., Edwards, A.R., Osborne, C.G., WO Patent Applications 96/04462, 96/29501, 96/29502 (1996).

Edwards, A.R., in *(First) International Conference on Natural Gas Hydrates*, *Ann. NY Acad. Sci.* (Sloan, E.D., Happel, J., et al., eds.), **715**, 543 (1994).

Freitas, A.M., Lobao, D., Anselmo C., Cardoso, C.B., in *Offshore Technology Conference Proceedings*, OTC 14257 Houston, TX, May (2002).

Fu, B., *Special Publication—Royal Society of Chemistry, Chemistry in the Oil Industry VII*, p. 264 (2002).

Gateau, P., Sinquin, A., Beunat, V., Vilagines, R., US Patent Application 2004/0162456 (2004).

Gudmundsson, J., Borrehaug, A., in *Proc. Second International Conference on Natural Gas Hydrates* (Monfort, J.P., ed.), Toulouse, France, June 2–6, p. 415 (1996).

Gudmundsson, J., Borrehaug, A., in *Proc. Third International Conference on Natural Gas Hydrates*, Salt Lake City, Utah, U.S.A., July 18–22, 1999; *Ann. NY Acad. Sci.* (Holder, G.D., Bishnoi, P.R., eds.), **912**, 403 (2000).

Hare, S., Case, R., Canyon Express Commissioning and Start-up Experience, in *Offshore Technology Conference Proceedings*, OTC15097, Houston, TX, May 6 (2003).

Hatton, G.J., Kruka, V.R., *Hydrate Blockage Formation—Analysis of Werner Bolley Field Test Data*, DeepStar CTR 5209-1 (2002).

Huo, Z., Freer, E., Lamar, M., Sannigrahi, B., Knauss, D.M., Sloan, E.D., *Chem. Eng. Sci.*, **56**, 4979 (2001).

ISP, Internal unpublished reports, cited in Kelland, 834 (2006).

Kalogerakis, N., Jamaluddin, A.K.M., Dhloabhai, P.D., Bishnoi, P.R., in *Proc. SPE International Symposium on Oilfield Chemistry*, SPE25188, New Orleans, LA, March 2–5, 375 (1993).

Katz, D.L., *Trans. AIME*, **160**, 140 (1945).

Kelland, M.A., *Energy Fuels*, **20**(3), 825 (2006).

Kelland, M.A., Svartaas, T.M., Ovsthus, T.M., in *Proc. Third International Conference on Natural Gas Hydrates*, Salt Lake City, Utah, U.S.A., July 18–22, 1999; *Ann. NY Acad. Sci*. (Holder, G.D., Bishnoi, P.R. eds.), **912**, 281 (2000).

Kent, R.P., Coolen, M.E., *Hydrates in Natural Gas Lines*, Mobil Internal Report (1992).

Kidnay, A.J., Parrish, W.R., *Fundamentals of Natural Gas Processing*, Taylor and Francis, Boca Raton, FL (2006).

King, R., et al., *Canadian Association of Petroleum Producers Hydrate Guidelines*, Canadian Association of Petroleum Producers, Calgary, Alberta, Canada (1994).

Klomp, U.C., WO Patent Application 99/13197 (1999).

Klomp, U.C., WO Patent Application 01/77270 (2001).

Klomp, U.C., Kruka, V.C., Reijnhart, R., WO Patent Application 95/17579 (1995).

Klomp, U.C., Reijnhart, R., WO Patent Application 96/34177 (1996).

Klug, P., Feustel, M., Frenz, V., WO Patent Application 98/22557 and 98/03615 (1998).

Kuhs, W.F., Genov, G., Stalkova, D.K., Hansen, T., *Phys. Chem. Chem. Phys.*, **6**, 4917 (2004).

Larsen, R., Makogon, T., Knight, C., Sloan, E.D., in *Proc. Second International Conference on Natural Gas Hydrates* (Monfort, J.P., ed.), Toulouse, France, June 2–6, p. 163 (1996).

Lee, D.J., Englezos, P., in *Proc Fifth International Conference on Gas Hydrates* (Austvik, T., ed.), Trondheim, Norway, June 13–16, p. 44 (2005).

Leporcher, E.M., Fourest, J.M., Labes Carrier, C., Lompre, M., in *Proc. 1998 SPE European Petroleum Conference*, SPE 50-683, The Hague, The Netherlands, October 20–22 (1998).

Lingelem, M.N., Majeed, A.I., Stange, E., in *(First) International Conference on Natural Gas Hydrates*, *Ann. NY Acad. Sci*. (Sloan, E.D., Happel, J., et al., eds.), **715**, 75 (1994).

Long, J., Lederhos, J., Sum, A., Christiansen, R., Sloan, E.D., "Kinetic Inhibitors of Natural Gas Hydrates," in *Proc. 73rd Annual Convention of Gas Processors Association*, New Orleans, LA, March 7–9, p. 85 (1994).

Makogon, Y.F., *Hydrates of Hydrocarbons*, PennWell Books, Tulsa, OK (1997).

Maximilian, A., Neubecker, K., Sanner, A., US Patent 6867262 (2005).

Mehta, A.P., Hebert, P.B., Cadena, E.R., Weatherman, J.P., *SPE Prod. Facil*., 73 (2003).

Mentor Subsea, *Methods to Clear Blocked Flowlines*, DeepStar CTR A208-1 (1996).

Milburn, C.R., Sitz, G.M., US Patent 644852 B1 (2002).

Muijs, H.M., Anselme, M. J., Beers, N.C.M., Van Os, N.M., Kind, C.E., Patent Application, Nr. 91.0619 (1991).

Nakajima, Y., Takaoki, T., Ohgaki, K., Ota, S., in *Proc. Fourth International Conference on Gas Hydrates* (Mori, Y.H., ed.), Yokohama, Japan, May 19–23, 987 (2002).

Namba, T., Fujii, Y., Saeki, R., Kobayashi, H., WO Patent Application 96/38492 and 96/37584 (1996).

Neubecker, K., Personal communication in 2005 to M.Kelland, cited in Kelland, p. 828 (2006).

Notz, P.K., in *(First) International Conference on Natural Gas Hydrates*, Annals of New York Academy of Sciences (Sloan, E.D., Happel, J., et al., eds.), **715**, 425 (1994).

Notz, P.K., Bumbgartner, S.B., Schaneman, B.D., Todd, J.L., in *Proc. 27th Ann OTC*, OTC 7777, Houston, TX, May 1–4 (1995).

Pakulski, M. European Patent Application 57458 (1998).

Pakulski, M. US Patent Application 6331508 (2001).

Palermo, T., Argo, C.B., Goodwin, S.P., Henderson, A., in *Proc. Third International Conference on Natural Gas Hydrates*, Salt Lake City, Utah, July 18–22, 1999; *Ann. NY Acad. Sci.* (Holder, G.D., Bishnoi, P.R., eds.), **912**, 355 (2000).

Palermo, T., Mussumeci, A., Leporcher, E., in *Proc. Offshore Technology Conference*, OTC 16681, Houston, TX, May 3–8 (2004).

Palermo, T., Sinquin, A., Dhulesia, H., Fourest, J.M., in *Proc. of Multiphase 1997*, BHR Group, p. 133 (1997).

Panchalingham, V., Rudel, M.G, Bodnar, S.H., US Patent Application 20050081714 (2005a).

Panchalingham, V., Rudel, M.G., Bodnar, S.H., US Patent Application 20050081432 (2005b).

Panchalingham, V., Rudel, M.G., Bodnar, S.H., US Patent Application 20050085396 (2005c).

Panchalingham, V., Rudel, M.G., Bodnar, S.H., US Patent Application 20050085675 (2005d).

Panchalingham, V., Rudel, M.G., Bodnar, S.H., US Patent Application 20050085676 (2005e).

Peters, D.J., *A Study of Hydrate Dissociation in Flowlines by the Method of Two-Sided Depressurization: Experiment and Model*, M.S. Thesis, Colorado School of Mines, Golden, CO (1999).

Pfeiffer, D.G., Costello, C.A, Talley, L.D., Wright, P.J., WO Patent Application 99/64718 (1999).

Philips, N.J., in *Proc. 8th International Oilfield Chemical Symposium* Geilo, Norway, March (1997).

Przbylinski, J.L., Rivers, G.T., US Patent 6596911 B2 (2003).

Reijnhout, M.J., Kind, C.E., Klomp, U.C., European Patent Application, 0 526 929 AL (1993).

Reynhout, M.J., Anselme, M.J., Beers, N.C.M., Van Os, N.M., Kind, C.E., Patent Application Nr. 91.0619 (1993).

Rivers, G.T., Crosby, D.L., US Patent Application 2004/0110998 (2004) WO Patent Application 2004/22909 (2004).

Rivers, G.T., Downs, H.H., US Patent Application 20040144732 (2004).

Rivers, G.T., Frostman, L.M., Pryzbyliski, J.L., McMahon, J.A., US Patent Application 2003146173 (2003).

Rogalands Research Unpublished Report of Early 1990s, cited in Kelland, p. 825 (2006).

Rogalands Research Unpublished Reports of 1995, cited in Kelland, p. 832 (2006).

Shirota, H., Aya, I., Namie, S., Bollavaram, P., Turner, D., Sloan, E.D., in *Proc. Fourth International Conference on Gas Hydrates* (Mori, Y.H., ed.), Yokohama, Japan, May 19–23, p. 972 (2002).

Sinquin, A., Vellyh, M., Durand, J.P., European Patent Application 789132 (1998).

Sloan, E.D., U.S. Patent 5,420,370, May 30 (1995a).

Sloan, E.D., U.S. Patent 5,432,292, July 11 (1995b).

Sloan, E.D., *Hydrate Engineering*, Monograph 21, Society of Petroleum Engineers, Richardson, TX (2000).

Sugier, A., Bourgmayer, P., Behar, E., Freund, E., European Patent Applications 323307, 323774 (1989).

Talley, L.D., Oelfke, R.H., WO Patent Application 97/07320 (1997).

Taylor, C.J., *Adhesion Force between Hydrate Particles and Macroscopic Investigation of Hydrate Film Growth at the Hydrocarbon/Water Interface*, M.Sc. Thesis, Colorado School of Mines, Golden, CO (2006).

Thieu, V., Bakeev, K., Shih, J.S., US Patent 6359047 (2002).

Todd, J.L., et al., *Reliabilty Engineering—Gas Freezing and Hydrates*, Texaco Company Hydrate Handbook, New Orleans, LA (1996).

Toyama, M., Seye, M., World Patent Application WO 02/10318 (2002).

Turner, D.J., *Clathrate Hydrate Formation in Water-in-Oil Dispersions*, Ph.D. Thesis, Colorado School of Mines, Golden, CO (2004).

Urdahl, O., Lund, A., Mork, P., Nilsen, T.-N., *Chem. Eng. Sci.*, **50**, 863 (1995).

Welling and Associates 1999 Survey, cited by Macintosh, N., "Flow Assurance Still Leading Concern Among Producers," *Offshore*, October (2000).

Wilson, A., Overaa, S.J., Holm, H., *Offshore Technology Conference*, OTC 1655, Houston, TX, May 3–6 (2004).

Wolden, M., Lund, A., Oza, N., Makogon, T., Argo, C.B., Larsen, R., in *Proc. Fifth International Conf. on Gas Hydrates* (Austvik, T., ed.), paper 4002 (5 volumes and CD), Trondheim, Norway, June 13–16, p. 1101 (2005).

Wright, J.F., Dallimore, S.D., Nixon, F.M., Dchesne, C., in *Scientific Results from the Mallik 2002 Gas Hydrate Production Research Well Program*, Mackenzie Delta, Northwest Territories, Canada (Dallimore, S.R., Collett, T.S., eds.), Geological Survey of Canada Bulletin 585, including CD, p. 92 (2005).

Yang, S.O., Kleehammer, D.M., Huo, Z., Sloan, E.D., Miller, K.T., *J. Colloid Interf. Sci.*, **277**, 335 (2004).

Yousif, M.H., Li, P.M., Selim, M.S., Sloan, E.D., *J. Inclus. Phenom. Mol.*, **8**, 71 (1990).